

**Spring temperature variability over Turkey since 1800 CE reconstructed
from a broad network of tree-ring data**

Nesibe Köse^{(1),*}, H. Tuncay Güner⁽¹⁾, Grant L. Harley⁽²⁾, Joel Guiot⁽³⁾

⁽¹⁾Istanbul University, Faculty of Forestry, Forest Botany Department 34473 Bahçeköy-Istanbul, Turkey

⁽²⁾University of Southern Mississippi, Department of Geography and Geology, 118 College Drive Box 5051, Hattiesburg, Mississippi, 39406, USA

⁽³⁾Aix-Marseille Université, CNRS, IRD, CEREGE UM34, ECCOREV, 13545 Aix-en-Provence, France

*Corresponding author. Fax: +90 212 226 11 13

E-mail address: nesibe@istanbul.edu.tr

Abstract

The meteorological observational period in Turkey, which starts *ca.* 1930 CE, is too short for understanding long-term climatic variability. Tree rings have been used intensively as proxy records to understand summer precipitation history of the region, primarily because of having a dominant precipitation signal. Yet,, the historical context of temperature variability is unclear. Here we used higher order principle components of a network of 23 tree-ring chronologies to provide a high-resolution spring (March–April) temperature reconstruction over Turkey during the period 1800–2002. The reconstruction model accounted for 67% (Adj. $R^2 = 0.64$, $p < 0.0001$) of the instrumental temperature variance over the full calibration period (1930–2002). The reconstruction is punctuated by a temperature increase during the 20th century; yet extreme cold and warm events during the 19th century seem to eclipse conditions during the 20th century.. We found significant correlations between our March–April spring temperature reconstruction and existing gridded spring temperature reconstructions for Europe over Turkey and southeastern Europe. Moreover, the precipitation signal obtained from the tree-ring network (first principle component) showed highly significant correlations with gridded summer drought index reconstruction over Turkey and Mediterranean countries. Our results showed that, beside the dominant precipitation signal, a temperature signal can be extracted from tree-ring series and they can be useful proxies to reconstruct past temperature variability.

KEYWORDS: Dendroclimatology, Climate reconstruction, *Pinus nigra*, Principle component analysis, Spring temperature.

1 Introduction

Long term meteorological observations in the Mediterranean region allow access to 100 years of instrumental recordings of temperature, precipitation and pressure in most of the region. Moreover, natural archives as well as documentary information provide resources with which to make sensitive climate reconstructions. An extensive body of literature details climate changes in the Mediterranean region over the last two millennia (Luterbacher et al. 2012). Paleolimnological studies provide evidence that the Medieval Climatic Anomaly (MCA; 900–1300 CE) characterized warm and dry conditions over the Iberian Peninsula, while the Little Ice Age (LIA; 1300–1850 CE) brought opposite climate conditions, forced by interactions between the East Atlantic and North Atlantic Oscillation (Sanchez-Lopez et al. 2016). In addition, Roberts et al. (2012) highlighted an intriguing spatial dipole NAO pattern between the western and eastern Mediterranean region, which brought anti-phased warm (cool) and wet (dry) conditions during the MCA and LIA. The hydro-climate patterns revealed by previous investigations appear to have been forced not only by NAO, but other climate modes with non-stationary teleconnections across the region (Roberts et al. 2012).

The climate of Turkey is mainly characterized by Mediterranean macro climate (Türkeş, 1996a). Contrary to the most countries in the Mediterranean region, Turkey has relatively short meteorological records, which start in the 1930s, for understanding long-term climatic variability. On the other hand, proxy records such as speleothems (Fleitmann et al. 2009, Jex et al. 2010, Göktürk et al. 2011), lake sediments (Wick et al. 2003, Jones et al. 2006, Roberts et al. 2008, 2012, Kuzucuoğlu et al. 2011, Woodbridge and Roberts 2011, Ülgen et al. 2012, Dean et

al. 2013) and tree-rings, have been used to reconstruct long term hydroclimate conditions over Turkey. Tree rings in particular have shown to provide useful information about the past climate of Turkey and were used intensively during the last decade to reconstruct precipitation in the Aegean (Griggs et al. 2007), Black Sea (Akkemik et al. 2005, 2008; Martin-Benitto et al. 2016), Mediterranean regions (Touchan et al. 2005a), as well as the Sivas (D'Arrigo & Cullen 2001), southwestern (Touchan et al. 2003, Touchan et al. 2007; Köse et al. 2013), south-central (Akkemik & Aras 2005) and western Anatolian (Köse et al. 2011) regions of Turkey. These studies used tree rings to reconstruct precipitation because available moisture is often found to be the most important limiting factor that influences radial growth of many tree species in Turkey. These studies revealed past spring-summer precipitation, and described past dry and wet events and their duration. Recently, Cook et al. (2015) presented Old World Drought Atlas (OWDA), which is a set of year by year maps of reconstructed Palmer Drought Severity Index from tree-ring chronologies over the Europe and Mediterranean Basin.

Besides detailed information on precipitation history represented by these paleoscientific studies, we have still very limited knowledge of past temperature variability of Turkey. For example, significant decreases in spring diurnal temperature ranges (DTR) occurred throughout Turkey from 1929 to 1999 (Turkes & Sumer 2004). This decrease in spring DTRs was characterized by day-time temperatures that remained relatively constant while a significant increase in night-time temperatures were recorded over western Turkey and were concentrated around urbanized and rapidly-urbanizing cities. The historical context of this gradual warming trend in spring temperatures is unclear. Heinrich et al. (2013) provided a winter-to-spring temperature proxy for Turkey from carbon isotopes within the growth rings of *Juniperus excelsa* M. Bieb. since AD

1125. Low-frequency temperature trends corresponding to the end of Medieval Climatic Anomaly and Little Ice Age were identified in the record, but the proxy failed to identify the recent warming trend during the 20th century. In this study, we present a tree-ring based spring temperature reconstruction from Turkey and compare our results to previous reconstructions of temperature and precipitation to provide a more comprehensive understanding of climate conditions during the 19th and 20th centuries.

2 Data and Methods

2.1 Climate of the Study Area

The study area, which spans 36–42° N and 26–38° E, was based on the distribution of available tree-ring chronologies. This vast area covers much of western Anatolia and includes the western Black Sea, Marmara, and western Mediterranean regions. Much of this area is characterized by a Mediterranean climate that is primarily controlled by polar and tropical air masses (Türkeş 1996a, Deniz et al. 2011). In winter, polar fronts from the Balkan Peninsula bring cold air that is centered in the Mediterranean. Conversely, the dry, warm conditions in summer are dominated by weak frontal systems and maritime effects. Moreover, the Azores high-pressure system in summer and anticyclonic activity from the Siberian high-pressure system often cause below normal precipitation and dry sub-humid conditions over the region (Türkeş 1999, Deniz et al. 2011). In this Mediterranean climate, annual mean temperature and precipitation range from 3.6 °C to 20.1 °C and from 295 to 2220 mm, respectively, both of which are strongly controlled by elevation (Deniz et al. 2011).

2.2 Development of tree-ring chronologies

To investigate past temperature conditions, we used a network of 23 tree-ring site chronologies (Fig. 1). Fifteen chronologies were produced by previous investigations (Mutlu et al. 2011, Akkemik et al. 2008, Köse et al. unpublished data, Köse et al. 2011, Köse et al. 2005) that focused on reconstructing precipitation in the study area. In addition, we sampled eight new study sites and developed tree-ring time series for these areas (Table 1). Increment cores were taken from living *Pinus nigra* Arnold and *Pinus sylvestris* L. trees and cross-sections were taken from *Abies nordmanniana* (Steven) Spach and *Picea orientalis* (L.) Link trunks.

Samples were processed using standard dendrochronological techniques (Stokes & Smiley 1968, Orvis & Grissino-Mayer 2002, Speer 2010). Tree-ring widths were measured, then visually crossdated using the list method (Yamaguchi 1991). We used the computer program COFECHA, which uses segmented time-series correlation techniques, to statistically confirm our visual crossdating (Holmes 1983, Grissino-Mayer 2001). Crossdated tree-ring time series were then standardized by fitting a 67% cubic smoothing spline with a 50% cutoff frequency to remove non-climatic trends related to the age, size, and the effects of stand dynamics using the ARSTAN program (Cook 1985, Cook et al. 1990a). These detrended series were then pre-whitened with low-order autoregressive models to produce time series with a strong common signal and without biological persistence. These series may be more suitable to understand the effect of climate on tree-growth, even if any persistence due to climate might be removed by pre-whitening. For each chronology, the individual series were averaged to a single chronology by

132 computing the biweight robust means to reduce the influences of outliers (Cook et al. 1990b). In
133 this research we used residual chronologies obtained from ARSTAN to reconstruct temperature.

134
135 The mean sensitivity, which is a metric representing the year-to-year variation in ring width
136 (Fritts 1976), was calculated for each chronology and compared. The minimum sample depth for
137 each chronology was determined according to expressed population signal (EPS), which we used
138 as a guide for assessing the likely loss of reconstruction accuracy. Although arbitrary, we
139 required the commonly considered threshold of $EPS > 0.85$ (Wigley et al. 1984; Briffa & Jones
140 1990).

142 2.3 Identifying relationship between tree-ring width and climate

143
144 We extracted high resolution monthly temperature and precipitation records from the climate
145 dataset CRU TS 3.23 gridded at 0.5° intervals (Jones and Harris 2008) from KNMI Climate
146 Explorer (<http://climexp.knmi.nl>) for $36\text{--}42^\circ\text{N}$, $26\text{--}38^\circ\text{E}$. The period AD 1930–2002 was
147 chosen for the analysis because it maximized the number of station records within the study area.

148
149 First, the climate-growth relationships were investigated with response function analysis (RFA)
150 (Fritts 1976) for biological year from previous October to current October using the
151 DENDROCLIM2002 program (Biondi & Waikul 2004). This analysis is done to determine the
152 months during which the tree-growth is the most responsive to temperature. RFA results showed
153 that precipitation from May to August and temperature in March and April have dominant
154 control on tree-ring formation in the area. Second, we produced correlation maps showing

correlation coefficients between tree-ring chronologies and the climate factors most important for tree growth, which are May–August precipitation and March–April temperature, to find the spatial structure of radial growth-climate relationship (St. George 2014, St. George and Ault 2014, Hellmann et al. 2016). For each site we used the closest gridded temperature and precipitation values.

2.4 Temperature reconstruction

The climate reconstruction is performed by regression based on the principal component (PCs) of the 23 chronologies within the study area. Principle Component Analysis (PCA) was done over the entire period in common to the tree-ring chronologies. The significant PCs were selected by stepwise regression. We combined forward selection with backward elimination setting $p < 0.05$ as entrance tolerance and $p < 0.10$ as exit tolerance. The final model obtained when the regression reaches a local minimum of the root mean squared error (RMSE). The order of entry of the PCs into the model was PC₃, PC₂₁, PC₄, PC₁₅, PC₅, PC₁₇, PC₇, PC₉, PC₁₀. The regression equation is calibrated on the common period (1930–2002) between robust temperature time-series and the selected tree-ring series. Third, the final reconstruction is based on bootstrap regression (Till and Guiot 1990), a method designed to calculate appropriate confidence intervals for reconstructed values and explained variance even in cases of short time-series. It consists in randomly resampling the calibration datasets to produce 1000 calibration equations based on a number of slightly different datasets.

The quality of the reconstruction is assessed by a number of standard statistics. The overall quality of fit of reconstruction is evaluated based on the determination coefficient (R^2), which expresses the percentage of variance explained by the model and RMSE, which expresses the calibration error. This does not insure the quality of the extrapolation which needs additional statistics based on independent observations, i.e. observations not used by the calibration (verification data). They are provided by the observations not resampled by the bootstrap process. The prediction RMSE (called RMSEP), the reduction of error (RE) and the coefficient of efficiency (CE) are calculated on the verification data and enable to test the predictive quality of the calibrated equations (Cook et al. 1994). Traditionally, a positive RE or CE values means a statistically significant reconstruction model, but bootstrap has the advantage to produce confidence intervals for such statistics without theoretical probability distribution and finally we accept the RE and CE for which the lower confidence margin at 95% are positive. This is more constraining than just accepting all positive RE and CE. For additional verification, we also present traditional split-sample procedure results that divided the full period into two subsets of equal length (Meko and Graybill 1995).

To identify the extreme March–April cold and warm events in the reconstruction, standard deviation (SD) values were used. Years one and two SD above and below the mean were identified as warm, very warm, cold, and very cold years, respectively. As a way to assess the spatial representation of our temperature reconstruction, we conducted a spatial field correlation analysis between reconstructed values and the gridded CRU TS3.23 temperature field (Jones and Harris 2008) for a broad region of the Mediterranean over the entire instrumental period (ca. 1930–2002). Finally, we compared our temperature reconstruction and also precipitation signal

(PC1) against existing gridded temperature and hydroclimate reconstructions for Europe over the period 1800–2002. We performed spatial correlation analysis between [1] our temperature reconstruction and gridded temperature reconstructions for Europe (Xoplaki et al. 2005, Luterbacher et al. 2016) and OWDA (Cook et al. 2015); and [2] PC1 and summer precipitation reconstruction (Pauling et al., 2006) and Old World Drought Atlas (OWDA) (Cook et al. 2015). To assess the significance of the correlation between our reconstruction (y) and gridded reconstructions ($x_j, j=1 \dots N$), we have calculated significance thresholds based on a Monte-Carlo technique. For each gridpoint j , we have calculated the correlation between x_j and y , but with a random permutation of the values of our reconstruction. This is repeated 1000 times with a different permutation. The 1000 correlation coefficients so obtained are expected to be zero as the correlation is established on non corresponding years. The 95th quantile of these 1000 coefficients is assumed to be passed in less than 5% of the cases. Then a correlation coefficient with a higher value is considered as positive with a 95% confidence. These thresholds are obtained with a common permutation for all x_j so that the spatial structure is conserved in the tests. The sign + is assigned to the x_j with a correlation higher than an expected value under the non-correlation hypothesis.

2 Results and Discussion

2.1 Tree-ring chronologies

In addition to 15 chronologies developed by previous studies, we produced six *P. nigra*, one *P. sylvestris*, one *A. nordmanniana* / *P. orientalis* chronologies for this study (Table 2). The Çorum district produced two *P. nigra* chronologies: one the longest (KAR; 627 years long) and the other the most sensitive to climate (SAH; mean sensitivity value of 0.25). Previous investigations of

climate-tree growth relationships reported a mean sensitivity range of 0.13–0.25 for *P. nigra* in Turkey (Köse 2011, Akkemik et al. 2008). The KAR, SAH, and ERC chronologies (with mean sensitivity values from 0.22 to 0.25) were classified as very sensitive, and the SAV, HCR, and PAY chronologies (mean sensitivity values range 0.17–0.18) contained values characteristic of being sensitive to climate. The lowest mean sensitivity value was obtained for the ART A. *nordmanniana* / *P. orientalis* chronology. Nonetheless, this chronology retained a statistically significant temperature signal ($p < 0.05$).

2.2 Tree-ring growth-climate relationship

RFA coefficients of May to August precipitation are positively correlated with most of the tree-ring series (Fig. 2) and among them, May and June coefficients are generally significant. The first principal component of the 23 chronologies, which explains 47% of the tree-growth variance, is highly correlated with May–August total precipitation, statistically ($r = 0.65$, $p < 0.001$) and visually (Fig. 3). The high correlation was expected given that numerous studies also found similar results in Turkey (Akkemik 2000a, Akkemik 2000b, Akkemik 2003, Akkemik et al. 2005, Akkemik et al. 2008, Akkemik & Aras 2005, Hughes et al. 2001, D'Arrigo & Cullen 2001, Touchan et al. 2003; Touchan et al. 2005a, Touchan et al. 2005b, Touchan et al. 2007, Köse et al. 2011, Köse et al. 2012, Köse et al. 2013, Martin-Benitto et al. 2016). The influence of temperature was not as strong as May–August precipitation on radial growth, although generally positive in early spring (March and April) (Fig. 2). Conversely, the ART chronology from northeastern Turkey contained a strong temperature signal, which was significantly positive in March.

Correlation maps representing influence of May-August precipitation (Fig. 4a) and March-April temperature (Fig 4b) also showed that strength of the summer precipitation signal is higher and significant almost all over the Turkey. Higher precipitation in summer has a positive effect on tree-growth, because of long-lasting dry and warm conditions over the Turkey (Türkeş 1996b, Köse et al. 2012). Spring precipitation signal are generally positive and significant only for four tree-ring sites. The sites located at the upper distributions of the species are generally showed higher correlations. The highest correlations obtained for *Picea/Abies* chronology (ART) from the Caucasus, and for *Pinus nigra* chronology (HCR) from the upper (about 1900 m) and southeastern distribution of the species. This black pine forest was still partly covered by snow from previous year during the field work in fall. Higher temperatures in spring maybe cause snow melt earlier and lead to produce larger annual rings. In addition to these chronologies, we also used the chronologies that revealed the influence of precipitation, as well as temperature to reconstruct March–April temperature.

2.3 March-April temperature reconstruction

The higher order PCs of the 23 chronologies are significantly correlated with the March–April temperature and, by nature, are independent on the precipitation signal (Table 3). The best selection for fit temperature are obtained with the PC₃, PC₄, PC₅, PC₇, PC₉, PC₁₀, PC₁₅, PC₁₇, PC₂₁, which explains together 25% of the tree-ring chronologies. So the temperature signal remains important in the tree-ring chronologies and can be reconstructed. The advantage to separate both signals through orthogonal PCs enable to remove an unwanted noise for our temperature reconstruction. Thus, PC₁ was not used as potential predictor of temperature because

it is largely dominated by precipitation (Table 3, Fig. 3). The last two PCs contain a too small part of the total variance to be used in the regressions. However, even if Jolliffe (1982) and Hadi & Ling (1998) claimed that certain PCs with small eigenvalues (even the last one), which are commonly ignored by principal components regression methodology, may be related to the independent variable, we must be cautious with that because they may be much more dominated by noise than the first ones. So, the contribution of each PC to the regression sum of squares is also important for selection of PCs (Hadi & Ling 1998). The findings of Jolliffe (1982) and Hadi & Ling (1998) provide a justification for using non-primary PCs, (*e.g.*, of second and higher order) in our regression, given that correlations with temperature may be over-powered by affects from precipitation in our study area (Cook 2011, personal communication).

Using this method, the calibration and verification statistics indicated a statistically significant reconstruction (Table 4, Fig. 5). For additional verification, we also present split-sample procedure results. Similarly bootstrap results, the derived calibration and verification tests using this method indicated a statistically significant RE and CE values (Table 5).

The regression model accounted for 67% ($\text{Adj. } R^2 = 0.64, p < 0.0001$) of the actual temperature variance over the calibration period (1930–2002). Also, actual and reconstructed March–April temperature values had nearly identical trends during the period 1930–2002 (Fig. 5). Moreover, the tree-ring chronologies successfully simulated both high frequency and warming trends in the temperature data during this period. The reconstruction was more powerful at classifying warm events rather than cold events. Over the last 73 years, eight of ten warm events in the instrumental data were also observed in the reconstruction, while five of nine cold events were

captured. Similarly, previous tree-ring based precipitation reconstructions for Turkey (Köse et al. 2011; Akkemik et al. 2008) were generally more successful in capturing dry years rather than wet years.

Our temperature reconstruction on the 1800–2002 period is obtained by bootstrap regression, using 1000 iterations (Fig. 6). The confidence intervals are obtained from the range between the 2.5th and the 97.5th percentiles of the 1000 simulations. Low frequency variability of our spring temperature reconstruction showed larger variability in nineteenth century than twentieth century. For the pre-instrumental period (1800–1929), a total of 23 cold (1813, 1818, 1821, 1824, 1837, 1848, 1854, 1858, 1860, 1869, 1877–1878, 1880–1881, 1883, 1897–1898, 1905–1907, 1911–1912, 1923) and 13 warm (1801–1802, 1807, 1845, 1853, 1866, 1872–1873, 1879, 1885, 1890, 1901, 1926) events were determined. After comparing our results with event years obtained from May–June precipitation reconstructions from western Anatolia (Köse et al. 2011), the cold years 1818, 1848, and 1897 appeared to coincide with wet years and 1881 was a very wet year for the entire region. Furthermore, these years can be described as cold (in March–April) and wet (in May–June) for western Anatolia.

Among the warm periods in our reconstruction, conditions during the year 1879 were dry, 1895 wet, and 1901 very wet across the broad region of western Anatolia (Köse et al. 2011). Hence, we defined 1879 as a warm (in March–April) and dry year (in May–June), and 1895 and 1901 were warm and wet years. In the years 1895 and 1901 the combination of a warm early spring and a wet late spring-summer caused enhanced radial growth in Turkey, interpreted as longer growing seasons without drought stress.

314
315 Of these event years, 1897 and 1898 were exceptionally cold and 1845, 1872 and 1873 were
316 exceptionally warm. During the last 200 years, our reconstruction suggests that the coldest year
317 was 1898 and the warmest year was 1873. The reconstructed extreme events also coincided with
318 accounts from historical records. Server (2008) recounted the winter of 1898 as characterized by
319 anomalously cold temperatures that persisted late into the spring season. A family, who brought
320 their livestock herds up into the plateau region in Kırşehir seeking food and water were suddenly
321 covered in snow on 11 March 1898. This account of a late spring freeze supports the
322 reconstruction record of spring temperatures across Turkey, and offers corroboration to the
323 quality of the reconstructed values.

324
325 Seyf (1985) reported that extreme summer temperature during the year 1873 resulted in
326 widespread crop failure and famine. Historical documents recorded an infamous drought-derived
327 famine that occurred in Anatolia from 1873 to 1874 (Quataert, 1996, Kuniholm, 1990), which
328 claimed the lives of 250,000 people and a large number of cattle and sheep (Faroghi, 2009). This
329 drought caused widespread mortality of livestock and depopulation of rural areas through human
330 mortality, and migration of people from rural to urban areas. Further, the German traveler
331 Naumann (1893) reported a very dry and hot summer in Turkey during the year 1873 (Heinrich
332 et al, 2013). Conditions worsened when the international stock exchanges crashed in 1873
333 (Zürcher, 2004). Our temperature record suggests that dry conditions during the early 1870s
334 were possibly exacerbated by warm spring temperatures that likely carried into summer. A
335 similar pattern of intensified drought by warm temperatures was demonstrated recently by
336 Griffin and Anchukaitis (2014) for the current drought in California, USA.

Extreme cold and warm events were usually one year long, and the longest extreme cold and warm events were two and three years, respectively. These results were similar with durations of extreme wet and dry events in Turkey (Touchan et al. 2003, Touchan et al. 2005a, Touchan et al. 2005b, Touchan et al. 2007, Akkemik & Aras, 2005, Akkemik et al. 2005, Akkemik et al. 2008, Köse et al. 2011, Güner et al. 2016). Moreover, seemingly innocuous short-term warm events, such as the 1807 event, were recorded across the Mediterranean and in high elevations of the European regions. Casty et al. (2005) reported the year 1807 as being one of the warmest alpine summers in the European Alps over the last 500 years. As such, a drought record from Nicault et al. (2008) echoes this finding, as a broad region of the Mediterranean basin experienced drought conditions.

Heinrich et al. (2013) analyzed winter-to-spring (January–May) air temperature variability in Turkey since AD 1125 as revealed from a robust tree-ring carbon isotope record from *Juniperus excelsa*. Although they offered a long-term perspective of temperature over Turkey, the reconstruction model, which covered the period 1949–2006, explained 27% of the variance in temperature since the year 1949. In this study, we provided a short-term perspective of temperature fluctuation based on a robust model (calibrated and verified 1930–2002; Adj. $R^2 = 0.64$; $p < 0.0001$). Yet, the Heinrich et al. (2013) temperature record did not capture the 20th century warming trend as found elsewhere (Wahl et al. 2010). However, their temperature trend does agree with trend analyses conducted on meteorological data from Turkey and other areas in

the eastern Mediterranean region. The warming trend seen during our reconstruction calibration period (1930–2002) was similar to the data shown by Wahl et al. (2010) across the region and hemisphere. Further, the warming trends seen in our record agrees with data presented by Turkes & Sumer (2004), of which they attributed to increased urbanization in Turkey. Considering long-term changes in spring temperatures, the 19th century was characterized by more high-frequency fluctuations compared to the 20th century, which was defined by more gradual changes and includes the beginning of decreased DTRs in the region (Turkes & Sumer 2004).

2.4 Comparison with instrumental gridded data and spatial reconstructions

Spatial correlation analysis revealed that our network-based temperature reconstruction was representative of conditions across Turkey, as well as the broader Mediterranean region (Fig. 7). During the period 1930–2002, estimated temperature values were highly significant (r range 0.5–0.6, $p < 0.01$) with instrumental conditions recorded from southern Ukraine to the west across Romania, and from northern areas of Libya and Egypt to the east across Iraq. The strength of the reconstruction model is evident in the broad spatial implications demonstrated by the temperature record. Thus, we interpret warm and cold periods and extreme events within the record with high confidence.

We compared our tree-ring based temperature reconstruction with existing gridded temperature reconstructions for Europe (Xoplaki et al. 2005, Luterbacher et al. 2016) and the Old World Drought Atlas (OWDA) (Cook et al. 2015) for further validation of the reconstruction (Fig. 8a, b, c, respectively). Spatial correlations over the past 200 years were lower with reconstructed

European summer temperature (May to July) (Fig. 8b). Yet, we expected this result because of the paucity of Turkey-derived proxies in the other reconstructions, as well as the differing seasons involved across the reconstructions. Similarly, our reconstruction showed weak correlations with summer drought index over Turkey. Beside comparing different seasons, perhaps this is because less precipitation begets drought conditions rather than high temperature in the region. The highest and significant ($p < 0.05$) correlations were found with European spring (March to May) temperature reconstruction over southeastern Europe, which are stronger over Turkey (Fig. 8a). We used the mean of corresponding grid points from European spring temperature reconstruction over the study area (36–42° N, 26–38° E) to show how the correlation changed over time (Fig. 9). The correlation coefficient was highly significant ($r = 0.76$, $p < 0.001$) during our calibration period (1930–2002). We found lower but still significant correlation ($r = 0.35$, $p < 0.10$) for the period of 1901–1929, which climatic records are very few over the region while available data has sufficient quality for most part of Europe. These results give additional verification for our reconstruction. Moreover, our reconstruction has a weak, insignificant relationship ($r = 0.13$, $p > 0.10$) during the 19th century. This may be related to poor reconstructive skill of European spring temperature reconstruction over Turkey, which contains few proxies from the country (Xoplaki et al. 2005, Luterbacher et al. 2004). Nonetheless, these results demonstrate that tree-ring chronologies from Turkey can serve as useful temperature proxies for further spatial temperature reconstructions to fill the gaps in the area.

We also compared the precipitation signal (PC1) obtained from our tree-ring network with Old World Drought Atlas (OWDA) (Cook et al. 2015) and gridded European summer precipitation reconstruction (Pauling et al., 2006) to test the strength of the signal spatially (Fig. 8d and e,

respectively). We calculated highly significant positive correlations with summer drought index over Turkey and neighboring European countries such as Greece, Bulgaria, and Romania, Italy while significant correlations are lower for the northern Mediterranean countries (Fig. 8d). These results showed that summer precipitation signal represented by PC1 is very strong not only on instrumental period, but also on pre-instrumental period, and represents a large spatial coverage. We found low and insignificant correlations over Turkey and Mediterranean countries with European summer precipitation reconstruction (Fig. 8e). Pauling et al. (2006) stated that poor reconstructive skills determined over Turkey because of few instrumental record before the 1930s.

4 Conclusions

In this study, we used a broad network of tree-ring chronologies to provide the first tree-ring based temperature reconstruction for Turkey and identified extreme cold and warm events during the period 1800–1929 CE. Similar to the precipitation reconstructions against which we compare our air temperature record, extreme cold and warm years were generally short in duration (one year) and rarely exceeded two-three years in duration. The coldest and warmest years over western Anatolia were experienced during the 19th century, and the 20th century is marked by a temperature increase.

Reconstructed temperatures for the 19th century suggest that more short-term fluctuations occurred compared to the 20th century. The gradual warming trend shown by our reconstruction calibration period (1930–2002) is coeval with decreases in spring DTRs. Given the results of

Turkes and Sumer (2004), the variations in short- and long-term temperature changes between the 19th and 20th centuries might be related to increased urbanization in Turkey.

We highlight that the 20th century warming trend is unprecedented within the context of the past *ca.* 200 years, especially over the past *ca.* 15 years. Correlations with gridded climate fields and other climate reconstructions from the region revealed that our network-based temperature reconstruction was representative of conditions across Turkey, as well as the broader Mediterranean region. Expanding the tree-ring network across Turkey, especially to the east, will improve the spatial implications of future temperature reconstructions.

The study revealed the potential for reconstructing temperature in an area previously thought impossible, especially given the strong precipitation signals displayed by most tree species growing in the dry Mediterranean climate that characterizes broad areas of Turkey. Our reconstruction only spans 205 years due to the shortness of the common interval for the chronologies used in this study, but the possibility exists to extend our temperature reconstruction further back in time by increasing the sample depth with more temperature-sensitive trees, especially from northeastern Turkey. Thus future research will focus on increasing the number of tree-ring sites across Turkey, and maximizing chronology length at existing sites that would ultimately extend the reconstruction back in time.

Acknowledgements

This research was supported by The Scientific and Technical Research Council of Turkey (TUBITAK); Projects ÇAYDAG 107Y267 and YDABAG 102Y063. N. Köse was supported by The Council of Higher Education of Turkey. We are grateful to the Turkish Forest Service personnel and Ali Kaya, Umut Ç. Kahraman and Hüseyin Yurtseven for their invaluable support during our field studies. We thank to Dr. Ufuk Turuncoğlu for his help on spatial analysis. J. Guiot was supported by the Labex OT-Med (ANR-11-LABEX-0061), French National Research Agency (ANR).

References

- Akkemik, Ü.: Dendroclimatology of Umbrella pine (*Pinus pinea* L.) in Istanbul (Turkey), *Tree-Ring Bull.*, 56, 17–20, 2000a.
- Akkemik, Ü.: Tree-ring chronology of *Abies cilicica* Carr. in the Western Mediterranean Region of Turkey and its response to climate, *Dendrochronologia*, 18, 73–81, 2000b.
- Akkemik, Ü.: Tree-rings of *Cedrus libani* A. Rich the northern boundary of its natural distribution, *IAWA J*, 24(1), 63–73, 2003.
- Akkemik, Ü. and Aras, A.: Reconstruction (1689–1994) of April–August precipitation in southwestern part of central Turkey, *Int. J. Clim.*, 25, 537–548, 2005.
- Akkemik, Ü., Dagdeviren, N., and Aras, A.: A preliminary reconstruction (A.D. 1635–2000) of spring precipitation using oak tree rings in the western Black Sea region of Turkey, *Int. J. Biomet.*, 49(5), 297–302, 2005.
- Akkemik, Ü., D’Arrigo, R., Cherubini, P., Köse, N., and Jacoby, G.: Tree-ring reconstructions of precipitation and streamflow for north-western Turkey, *Int. J. Clim.*, 28, 173–183, 2008.
- Biondi, F. and Waikul, K.: DENDROCLIM2002: A C++ program for statistical calibration of climate signals in tree-ring chronologies, *Comp. Geosci.*, 30, 303–311, 2004.
- Briffa, K. R. and Jones, P. D.: Basic chronology statistics and assessment. In: *Methods of Dendrochronology: Applications in the Environmental Sciences* (Cook, E. and Kairiukstis, L. A. eds). Kluwer Academic Publishers, Amsterdam, pp. 137–152, 1990.

482 Casty, C., Wanner, H., Luterbacher, J., Esper, J., and Böhm, R.: Temperature and precipitation
 483 variability in the European Alps since 1500, *Int. J. Clim.*, 25(14), 1855–1880, 2005.

484 Cook, E.: A time series analysis approach to tree-ring standardization. PhD. Dissertation.
 485 University of Arizona, Tucson, 1985.

486 Cook, E., Briffa, K., Shiyatov, S., and Mazepa, V.: Tree-ring standardization and growth-trend
 487 estimation. In: *Methods of Dendrochronology: Applications in the Environmental Sciences*
 488 (Cook, E. and Kairiukstis, L. A. eds). Kluwer Academic Publishers, Amsterdam, pp.104–
 489 122, 1990a.

490 Cook, E., Shiyatov, S., and Mazepa, V.: Estimation of the mean chronology. In: *Methods of*
 491 *Dendrochronology: Applications in the Environmental Sciences* (Cook, E. and Kairiukstis, L.
 492 A. eds). Kluwer Academic Publishers, Amsterdam, pp. 123–132, 1990b.

493 Cook, E.R, Seager R., et al.: Old World megadroughts and pluvials during the Common Era, *Sci.*
 494 *Adv.*, 1, e1500561, doi:10.1126/sciadv.1500561, 2015.

495 D'Arrigo, R. and Cullen, H. M.: A 350-year (AD 1628–1980) reconstruction of Turkish
 496 precipitation. *Dendrochronologia*, 19(2), 169–177, 2001.

497 Dean, R. J., Jones, M. D., et al.: Palaeo-seasonality of the last two millennia reconstructed from
 498 the oxygen isotope composition of carbonates and diatom silica from Nar Gölü, central
 499 Turkey, *Quat. Sci. Rev.*, 66, 35–44, 2013.

500 Deniz, A., Toros, T., and Incecik, S.: Spatial variations of climate indices in Turkey, *Int. J.*
 501 *Clim.*, 31, 394–403, 2011.

502 Fleitmann, D., Cheng, H., et al.: Timing and climatic impact of Greenland interstadials recorded
 503 in stalagmites from northern Turkey, *Geophys. Res. Lett.* 36, L19707. doi:
 504 10.1029/2009gl040050, 2009.

505 Fritts, H. C.: *Tree Rings and Climate*. Academic Press, New York, 1976.

506 Gokturk, O.M., Fleitmann, D., Badertscher, S., Cheng, H., Edwards, R.L., Tuysuz, O.:
 507 Climate on the Southern Black Sea coast during the Holocene, *Quat. Sci. Rev.*, 30, 2433–2445,
 508 2010.

509 Griggs, C., DeGaetano, A., Kuniholm, P., and Newton, M.: A regional high-frequency
 510 reconstruction of May–June precipitation in the north Aegean from oak tree rings, A.D.
 511 1809–1989, *Int. J. Clim.*, 27, 1075–1089, 2007.

512 Grissino-Mayer, H. D.: Evaluating crossdating accuracy: A manual and tutorial for the computer
 513 program COFECHA, *Tree-Ring Res.*, 57, 205–221, 2001.

514 Griffin, D. and Anchukaitis, K. J.: How unusual is the 2012–2014 California drought? *Geophys.*
 515 *Res. Lett.*, 41(24), 9017–9023, 2014.

516 Güner, H.T., Köse, N., Harley, G. L.: 200-year reconstruction of Kocasu River (Sakarya River
 517 Basin, Turkey) streamflow derived from a tree-ring network, *Int. J. Biometeorol.*, DOI
 518 10.1007/s00484-016-1223-y, 2016.

519 Hadi, A. S. and Ling, R. F.: Some cautionary notes on the use of principal components
 520 regression, *Amer. Statist.*, 52(1), 15–19, 1998.

521 Heinrich, I., Touchan, R., Liñán, I. D., Vos, H., and Helle, G.: Winter-to-spring temperature
 522 dynamics in Turkey derived from tree rings since AD 1125, *Clim. Dynam.*, 41(7–8), 1685–
 523 1701, 2013.

524 Hellmann, L., Agafonov, L., et al.: Diverse growth trends and climate responses across Eurasia's
 525 boreal forest. *Environmental Research Letters*: 11: 074021, doi:10.1088/1748-
 526 9326/11/7/074021.

527 Holmes, R. L.: Computer-assisted quality control in tree-ring data and measurements, *Tree-Ring*
 528 *Bull.*, 43, 69–78, 1983.

529 Hughes, M. K., Kuniholm, P. I., Garfin, G. M., Latini, C., and Eischeid, J.: Aegean tree-ring
 530 signature years explained, *Tree-Ring Res.*, 57(1), 67–73, 2001.

531 Jolliffe, I. T.: A note on the use of principal components in regression, *Appl. Stat.*, 31(3), 300–
 532 303, 1982.

533 Jex, C.N., Baker, A., et al.: Calibration of speleothem $\delta^{18}\text{O}$ with instrumental climate records
 534 from Turkey, *Global Planet. Change*, 71, 207–217, 2010.

535 Jones, M.D., Roberts, N., Leng, M.J., Türkeş, M.: A high-resolution late Holocene lake isotope
 536 record from Turkey and links to North Atlantic and monsoon climate, *Geology*, 34 (5), 361–
 537 364, 2006.

538 Jones, P. D. and Harris, I.: Climatic Research Unit (CRU) time-series datasets of variations in
 539 climate with variations in other phenomena. NCAS British Atmospheric Data Centre, 2008.
 540 <http://catalogue.ceda.ac.uk/uuid/3f8944800cc48e1cbc29a5ee12d8542d>

541 Köse, N., Akkemik, Ü., and Dalfes, H. N.: Anadolu'nun iklim tarihinin son 500 yılı:
 542 Dendroklimatolojik ilk sonuçlar. *Türkiye Kuvaterner Sempozyumu-TURQUA-V*, 02–03
 543 Haziran 2005, *Bildiriler Kitabı*, 136–142 (In Turkish), 2005.

544 Köse, N., Akkemik, Ü., Dalfes, H. N., and Özeren, M. S.: Tree-ring reconstructions of May–June
 545 precipitation of western Anatolia, *Quat. Res.*, 75, 438–450, 2011.

546 Köse, N., Akkemik, Ü., Dalfes, H. N., and Özeren, M. S., Tolunay D.: Tree-ring growth of *Pinus*
 547 *nigra* Arn. subsp. *pallasiana* under different climate conditions throughout western Anatolia,
 548 *Dendrochronologia*, 295-301, 2012.

549 Köse, N., Akkemik, U., Guner, H.T., Dalfes, H.N., Grissino-Mayer, H.D., Ozeren, M.S., Kindap,
 550 T.: An improved reconstruction of May– June precipitation using tree-ring data from western
 551 Turkey and its links to volcanic eruptions, *Int. J. Biometeorol*, 57(5), 691–701, 2013.

552 Kuzucuoğlu, C., Dörfler, W., Kunesch, S., Goupille, F.: Mid- to late-Holocene climate change in
 553 central Turkey: the Tecer Lake record, *Holocene*, 21, 173–188, 2011.

554 Luterbacher, J., Dietrich, D., Xoplaki, E., Grosjean, M., Wanner, H.: European seasonal and
 555 annual temperature variability, trends and extremes since 1500. *Science*, 303, 1499–1503,
 556 2004.

557 Luterbacher, J., R. García-Herrera, et al.: A review of 2000 years of paleoclimatic evidence in
 558 the Mediterranean. In: Lionello, P. (Ed.), *The Climate of the Mediterranean region: from the*
 559 *past to the future*. Elsevier, Amsterdam, The Netherlands, 87-185, 2012.

560 Luterbacher, J., Werner, J.P., et al.: European summer temperatures since Roman times.
 561 *Environmental Research Letters*, 11: 024001, doi:10.1088/1748-9326/11/1/024001, 2016.

562 Martin-Benito, D., Ummenhofer C.C., Köse, N., Güner, H.T., Pederson, N.: Tree-ring
 563 reconstructed May-June precipitation in the Caucasus since 1752 CE, *Clim. Dyn.*, DOI
 564 10.1007/s00382-016-3010-1, 2016.

565 Meko, D. M. and Graybill, D. A.: Tree-ring reconstruction of upper Gila River discharge, *Wat.*
 566 *Res. Bull.*, 31, 605–616, 1995.

567 Mutlu, H., Köse, N., Akkemik, Ü., Aral, D., Kaya, A., Manning, S. W., Pearson, C. L., and
 568 Dalfes, N.: Environmental and climatic signals from stable isotopes in Anatolian tree rings,
 569 Turkey, Reg. Environ. Change, doi: 10.1007/s1011301102732, 2011.

570 Nicault, A., Alleaume, S., Brewer, S., Carrer, M., Nola, P., and Guiot, J.: Mediterranean drought
 571 fluctuation during the last 500 years based on tree-ring data, *Clim. Dynam.*, 31(2–3), 227–
 572 245, 2008.

573 Orvis, K. H. and Grissino-Mayer, H. D.: Standardizing the reporting of abrasive papers used to
 574 surface tree-ring samples, *Tree-Ring Res.*, 58, 47–50, 2002.

575 Pauling, A., Luterbacher, J., Casty, C., Wanner, H.: Five hundred years of gridded high-
 576 resolution precipitation reconstructions over Europe and the connection to large-scale
 577 circulation. *Clim. Dynam.*, 26, 387–405, 2006.

578 Roberts, N., Jones, M.D., et al.: Stable isotope records of Late Quaternary climate and hydrology
 579 from Mediterranean lakes: the ISOMED synthesis, *Quat. Sci. Rev.*, 27, 2426–2441, 2008.

580 Roberts, N., Moreno, A., Valero-Garces, B.L.: Palaeolimnological evidence for an east-west
 581 climate see-saw in the Mediterranean since AD 900. *Glob. Planet. Change*, 84, 23–34, 2012.

582 Sanchez-López, G. Hernandez, A., Pla-Rabes, et al.: Climate reconstruction for the last two
 583 millennia in central Iberia: The role of East Atlantic (EA), North Atlantic Oscillation (NAO)
 584 and their interplay over the Iberian Peninsula. *Quaternary Science Reviews*, 149, 135–150,
 585 2016.

586 Server, M.: Evaluation of an oral history text in the context of social memory and traditional
 587 activity, *Milli Folklor* 77, 61–68 (In Turkish), 2008.

588 Speer, J. H.: *Fundamentals of Tree-Ring Research*, University of Arizona Press, Tucson, 2010.

589 St. George, S.: An overview of tree-ring width records across the Northern Hemisphere, *Quat.*
 590 *Sci. Rev.*, 95, 132–150, 2014.

591 St. George, S., and Ault, T. R.: The imprint of climate within northern hemisphere trees, *Quat.*
 592 *Sci. Rev.*, 89, 1–4, 2014.

593 Stokes, M. A. and Smiley, T. L.: *An Introduction to Tree-ring Dating*, The University of Arizona
 594 Press, Tucson, 1996.

595 Till, C. and Guiot, J.: Reconstruction of precipitation in Morocco since A D 1100 based on
 596 *Cedrus atlantica* tree-ring widths, *Quat. Res.*, 33, 337–351, 1990.

597 Touchan, R., Garfin, G. M., Meko, D. M., Funkhouser, G., Erkan, N., Hughes, M. K., and
 598 Wallin, B. S.: Preliminary reconstructions of spring precipitation in southwestern Turkey
 599 from tree-ring width, *Int. J. Clim.*, 23, 157–171, 2003.

600 Touchan, R., Xoplaki, E., Funkhouser, G., Luterbacher, J., Hughes, M. K., Erkan, N., Akkemik,
 601 Ü., and Stephan, J.: Reconstruction of spring/summer precipitation for the Eastern
 602 Mediterranean from tree-ring widths and its connection to large-scale atmospheric
 603 circulation, *Clim. Dynam.*, 25, 75–98, 2005a.

604 Touchan, R., Funkhouser, G., Hughes, M. K., and Erkan, N.: Standardized Precipitation Index
 605 reconstructed from Turkish ring widths, *Clim. Change*, 72, 339–353, 2005b.

606 Touchan, R., Akkemik, Ü., Huges, M. K., and Erkan, N.: May–June precipitation reconstruction
 607 of southwestern Anatolia, Turkey during the last 900 years from tree-rings, *Quat. Res.*, 68,
 608 196–202, 2007.

609 Turkes, M.: Spatial and temporal analysis of annual rainfall variations in Turkey, *Int. J. Clim.*,
 610 16, 1057–1076, 1996a.

611 Turkes, M.: Meteorological drought in Turkey: a historical perspective, 1930–1993. In: Drought
 612 Network News, International Drought Information Center, University of Nebraska, 8, pp. 17–
 613 21, 1996b.

614 Turkes, M.: Vulnerability of Turkey to desertification with respect to precipitation and aridity
 615 conditions. *Turk. J. Engineer. Environ Sci.*, 23, 363–380, 1999.

616 Turkes, M. and Sumer, U. M.: Spatial and temporal patterns of trends variability in diurnal
 617 temperature ranges of Turkey. *Theor. Appl. Clim.*, 77, 195–227, 2004.

618 Ülgen, U. B., Franz, S. O., Biltekin, D., Çagatay, M. N., Roeser, P. A., Doner, L., Thein, J.:
 619 Climatic and environmental evolution of Lake Iznik (NW Turkey) over the last ~ 4700 years,
 620 *Quatern. Int.*, 274, 88-101, 2012.

621 Xoplaki, E., Luterbacher J., Paeth H., Dietrich, D., Grosjean, M., Wanner, H.: European spring
 622 and autumn temperature variability and change of extremes over the last half millennium.
 623 *Geophys. Res. Lett.*, 32, L15713, doi:10.1029/2005GL023424.

624 Wahl, E. R., Anderson, D. M., Bauer, B. A., Buckner, R., Gille, E. P., Gross, W. S., Hartman,
 625 M., and Shah, A.: An archive of high-resolution temperature reconstructions over the past
 626 two millennia, *Geochem. Geophys. Geosyst.*, 11, Q01001, doi:10.1029/2009GC002817,
 627 2010.

628 Wick, L., Lemcke, G., Sturm, M.: Evidence of Lateglacial and Holocene climatic change and
 629 human impact in eastern Anatolia: high-resolution pollen, charcoal, isotopic and geochemical
 630 records from the laminated sediments of Lake Van, Turkey, *Holocene*, 13, 665–675, 2003.

631 Wigley, T. M. L., Briffa, K. R., and Jones, P. D.: On the average value of correlated time series
 632 with applications in dendroclimatology and hydrometeorology, *J. Clim. Appl. Met.*, 23, 201–
 633 213, 1984.

- 634 Woodbridge, J., Roberts, N.: Late Holocene climate of the Eastern Mediterranean inferred from
635 diatom analysis of annually-laminated lake sediments, *Quat. Sci. Rev.*, 30, 3381–3392, 2011.
- 636 Yamaguchi, D. K.: A simple method for cross-dating increment cores from living trees. *Can. J.*
637 *For. Res.*, 21, 414–416, 1991.
- 638 Zücher, E. J.: *Turkey: A modern history*. Oxford Publishing Services, New York, 2004.

639 Table 1. Site information for the new chronologies developed by this study in Turkey.

Site name	Site code	Species	No. trees/ cores	Aspect	Elev. (m)	Lat. (N)	Long. (E)
Çorum, Kargı, Karakise kayalıkları	KAR	<i>Pinus nigra</i>	22 / 38	SW	1522	41°11'	34°28'
Çorum, Kargı, Şahinkayası mevki	SAH	<i>P. nigra</i>	12 / 21	S	1300	41°13'	34°47'
Bilecik, Muratdere	ERC	<i>P. nigra</i>	12 / 25	SE	1240	39°53'	29°50'
Bolu, Yedigöller, Ayıkaya mevki	BOL	<i>P. sylvestris</i>	10 / 20	SW	1702	40°53'	31°40'
Eskişehir, Mihalıççık, Savaş alanı mevki	SAV	<i>P. nigra</i>	10 / 18	S	1558	39°57'	31°12'
Kayseri, Aladağlar milli parkı, Hacer ormanı	HCR	<i>P. nigra</i>	18 / 33	S	1884	37°49'	35°17'
Kahramanmaraş, Göksun, Payanburnu mevki	PAY	<i>P. nigra</i>	10 / 17	S	1367	37°52'	36°21'
Artvin, Borçka, Balcı işletmesi	ART	<i>Abies nordmanniana</i> <i>Picea orientalis</i>	23 / 45	N	1200– 2100	41°18'	41°54'

640

641

642 Table 2. Summary statistics for the new chronologies developed by this study in Turkey.

Site Code	Total chronology			Common interval		
	Time span	1st year (*EPS > 0.85)	Mean sensitivity	Time span	Mean correlations: among radii /between radii and mean	Variance explained by PC1 (%)
KAR	1307– 2003	1620	0.22	1740–1994	0.38 / 0.63	41
SAH	1663– 2003	1738	0.25	1799–2000	0.42 / 0.67	45
ERC	1721– 2008	1721	0.23	1837–2008	0.45 / 0.69	48
BOL	1752– 2009	1801	0.18	1839–1994	0.32 / 0.60	36
SAV	1630– 2005	1700	0.17	1775–2000	0.33 / 0.60	38
HCR	1532– 2010	1704	0.18	1730–2010	0.38 / 0.63	40
PAY	1537– 2010	1790	0.18	1880–2010	0.28 / 0.56	32
ART	1498– 2007	1624	0.12	1739–1996	0.37 / 0.60	41

643 *EPS = Expressed Population Signal [Wigley et al., 1984]

644

Table 3. Principal components analysis statistics for the Turkey temperature reconstruction model.

	Explained variance (%)	Correlation coefficients with		The chronologies represented by higher magnitudes** in the eigenvectors
		May–August PPT	March–April TMP	
PC1	46.57	0.65	0.19	KAR, KIZ, TEF, BON, USA, TUR, CAT, INC, ERC, YAU, SAV, TAN, SIU
PC2	7.86	–0.07	0.15	KAR, SAV, TIR, BOL, YAU, ESK, TEF, BON, SIU
PC3*	4.93	0.04	–0.48	HCR, PAY, BOL, YAU, SIA
PC4*	4.68	0.11	0.17	TEF, KEL, FIR, SIA, KIZ, SIU, ART
PC5*	4.42	–0.25	0.27	SAH, TIR, FIR, ART
PC6	3.73	0.15	–0.14	KIZ, FIR, SAV, KAR, TIR, PAY, ESK, TEF, BON, ART
PC7*	3.56	0.19	0.18	KIZ, BON, BOL, YAU, HCR, PAY, INC
PC8	2.87	0.26	0.01	HCR, ESK, BON, FIR, ERC, SIA
PC9*	2.45	0.16	0.17	PAY, USA, BOL, YAU, TIR, HCR, FIR, SIA, SIU
PC10*	2.21	0.14	–0.08	TUR, CAT, SAV, SIA, KEL, ERC, SIU
PC11	2.09	–0.36	–0.20	HCR, TEF, USA, INC, PAY, TUR, SAV, SIU
PC12	1.80	–0.12	0.05	TEF, CAT, YAU, HCR, ESK, USA, BOL, SIA
PC13	1.63	–0.06	0.17	TEF, TUR, BOL, KAR, YAU, SIA
PC14	1.55	–0.14	0.06	TIR, USA, FIR, TUR, YAU, KAR, BON
PC15*	1.50	–0.20	–0.14	KIZ, BON, USA, ESK, INC, BOL
PC16	1.31	0.04	0.08	SAH, HCR, INC, YAU, SAV, KAR, FIR, BOL, SIU
PC17*	1.25	0.15	0.19	SAH, SIU, KAR, ESK, TUR, ERC
PC18	1.14	0.13	0.02	KAR, TEF, TUR, SAV, BON, CAT
PC19	1.09	0.16	–0.11	PAY, INC, SAV, HCR, KEL, CAT, TAN
PC20	0.95	–0.15	–0.01	TIR, SAH, CAT
PC21*	0.89	0.06	–0.28	TUR, INC, TIR, SAV
PC22	0.85	0.44	0.10	KIZ, SAH, BON, YAU, SIU
PC23	0.67	–0.22	–0.02	TAN, KEL, TUR, CAT

“*” indicates the PCs, which used in the reconstruction as predictors

“**” which exceed ± 0.2 value.

Table 4. Calibration and verification statistics of bootstrap method (1000 iterations applied) showing the mean values based on the 95% confidence interval (CI).

Mean (95% CI)		
Calibration	RMSE	0.65 (0.52; 0.77)
	R^2	0.73 (0.60; 0.83)
Verification	RE	0.54 (0.15; 0.74)
	CE	0.51 (0.04; 0.72)
	RMSEP	0.88 (0.67; 1.09)

RMSE root mean squared error; R^2 coefficient of determination; *RE* reduction of error; *CE* coefficient of efficiency; *RMSEP* root mean squared error prediction

Table 5. Calibration and cross-validation statistics for the Turkey temperature reconstruction model.

Calibration Period	Verification Period	Adj. R^2	F	RE	CE
1930–1966	1967–2002	0.55	5.91	0.64	0.58
$p < 0.0001$					
1967–2002	1930–1966	0.71	10.45	0.63	0.46
$p < 0.0001$					

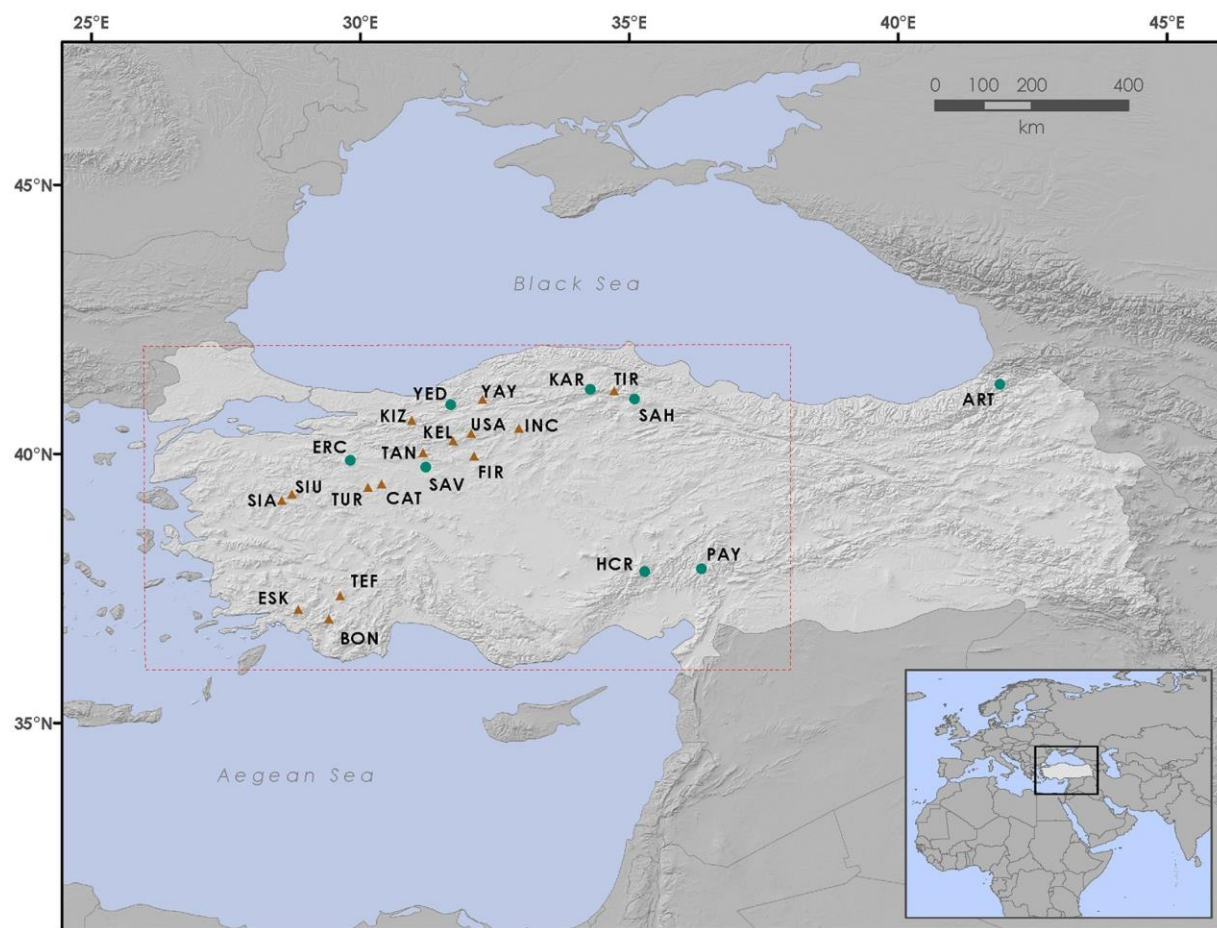


Figure 1. Tree-ring chronology sites in Turkey used to reconstruct temperature. Circles represent the new sampling efforts from this study and the triangles represent previously-published chronologies (YAY, SIA, SIU: Mutlu et al. 2011; TIR: Akkemik et al. 2008; TAN: Köse et al. unpublished data; KIZ, ESK, TEF, BON, KEL, USA, FIR, TUR: Köse et al. 2011; CAT, INC: Köse et al. 2005). The box (dashed line) represents the area for which the temperature reconstruction was performed.

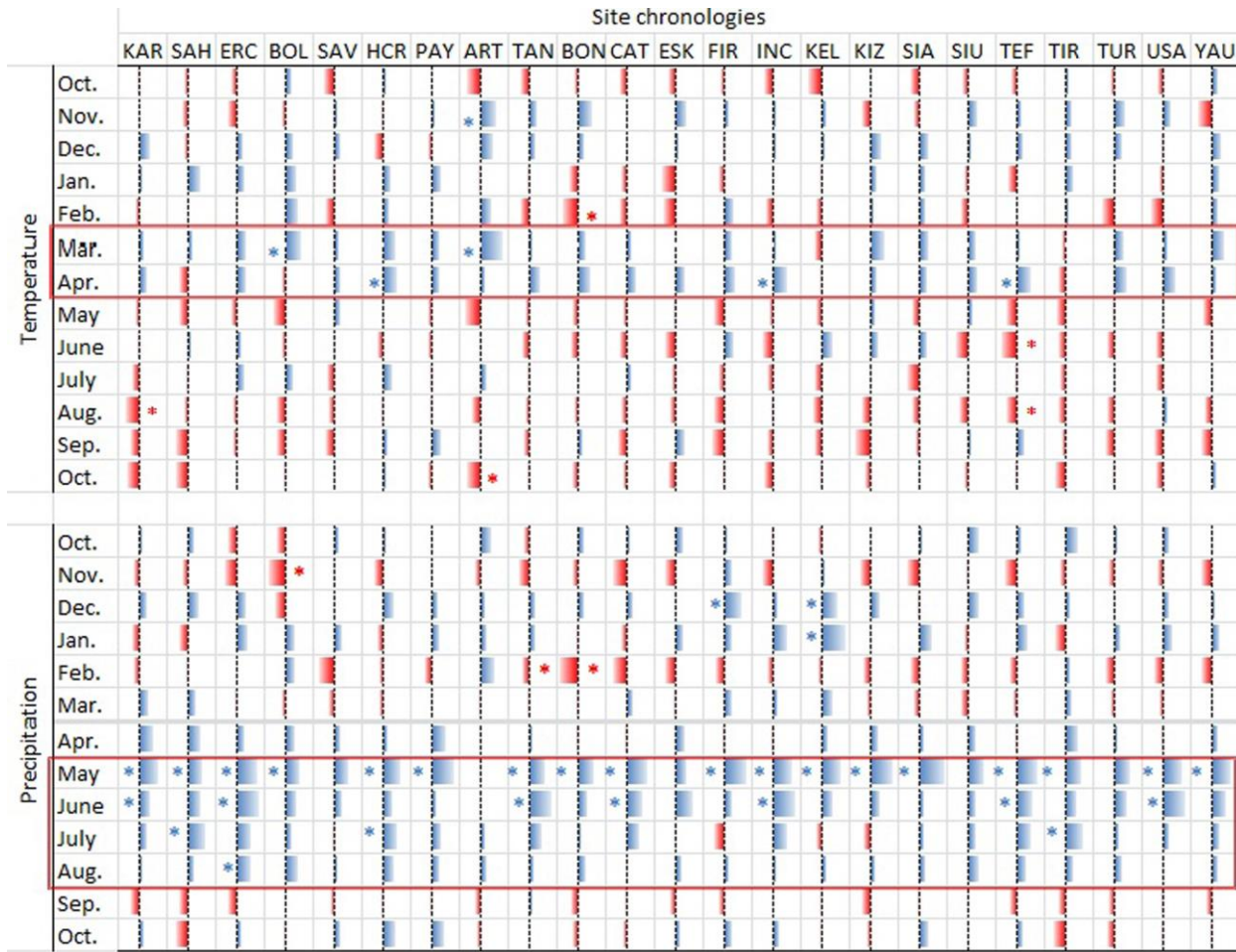


Figure 2. Summary of response function results of 23 chronologies. Red color represents negative effects of climate variability on tree ring width; blue color represents positive effects of climate variability on tree ring width. “*” indicates statistically significant response function confidents ($p < 0.05$). Each response function includes 13 weights for average monthly temperatures and 13 monthly precipitations from October of the prior year to October of current year.

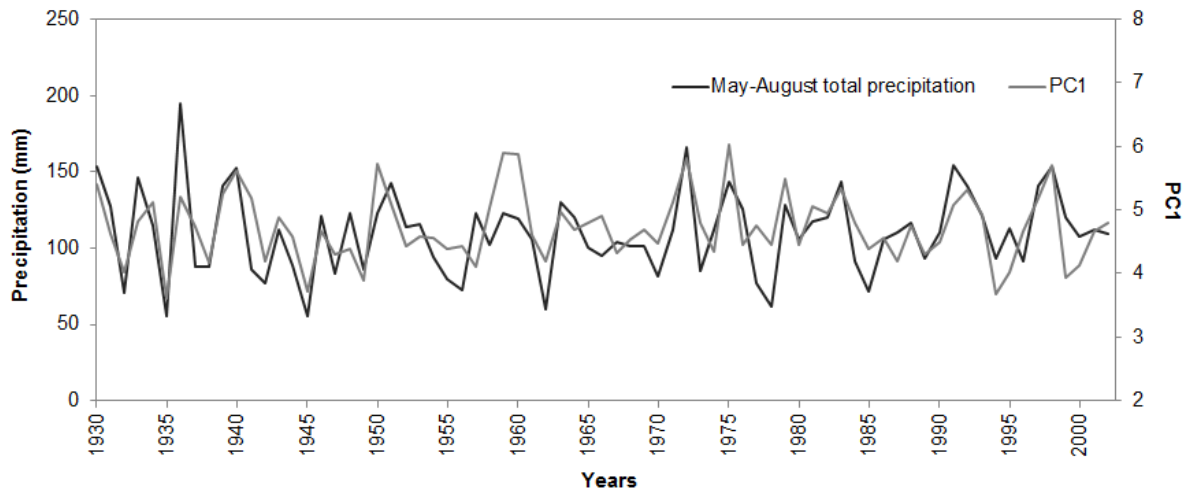


Figure 3. The comparison of May–August total precipitation (black) and the first principal component of 23 tree-ring chronologies (gray). Correlation coefficient between two time series is 0.65 ($p < 0.001$).

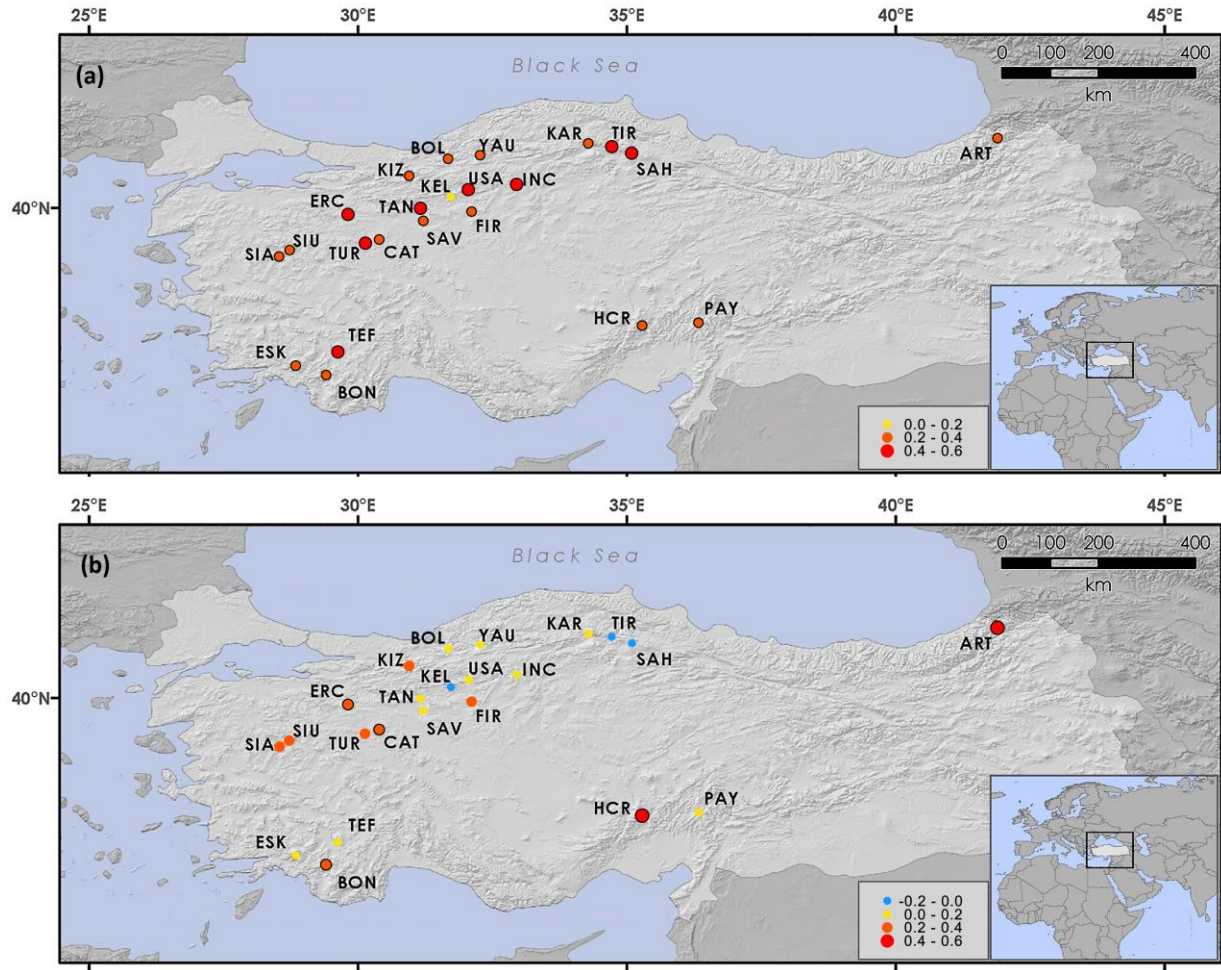


Figure 4. Maps showing Pearson's correlation coefficients between the sites chronologies and (a) May–August total precipitation and (b) March–April mean temperature for the period 1930–2012. For each site, the closest gridded ($0.5^\circ \times 0.5^\circ$) climate data obtained from CRU dataset were used. Graduated circle size and color correspond to correlation coefficient versus the climate variable. Black lines surrounding circles represent significant correlation coefficients ($p < 0.05$).

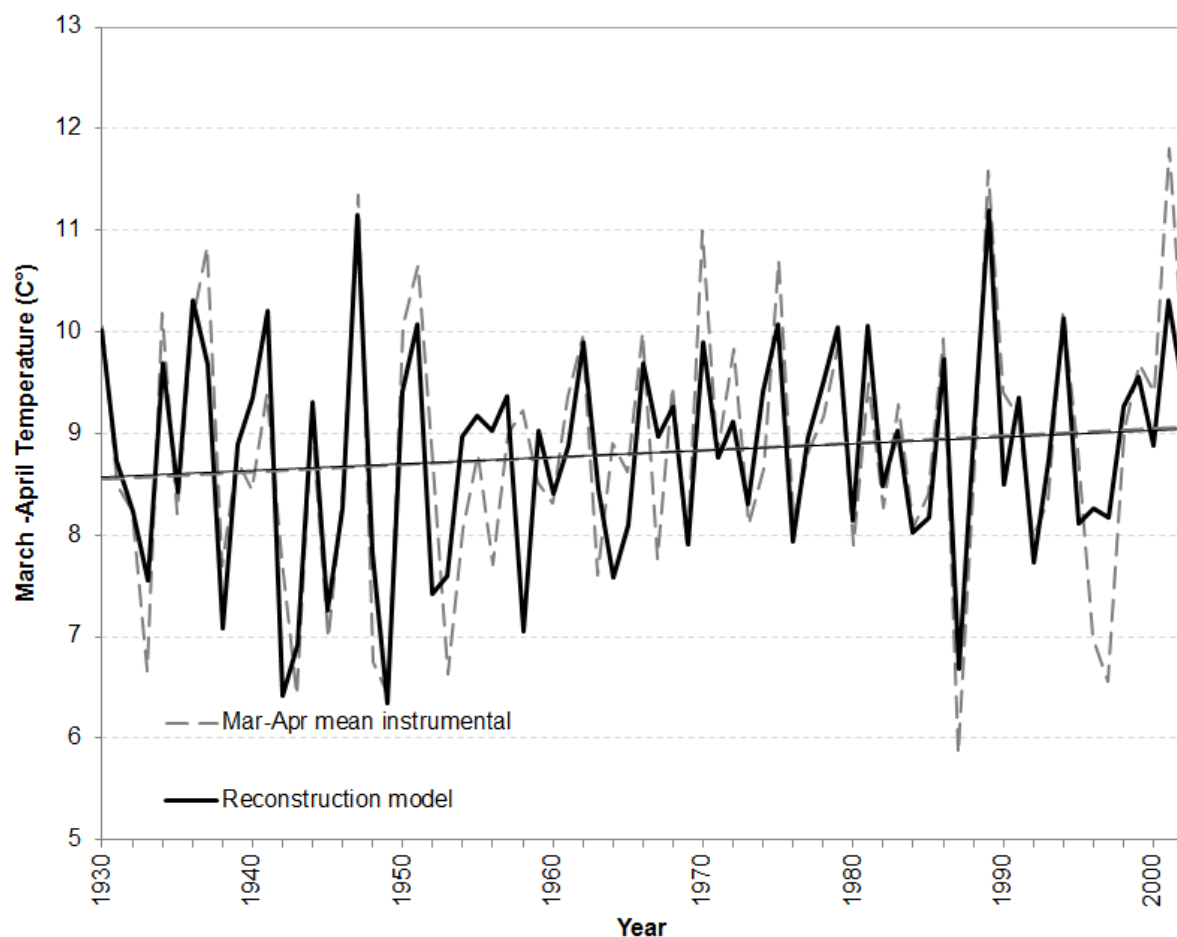


Figure 5. Actual (instrumental) and reconstructed March–April temperature (°C). Dashed lines (dark grey) represent actual values and solid lines (black) represent reconstructed values shown with trend lines (linear dashed grey and linear black lines, respectively). The tendency to warm up at the reconstructed temperature is in good agreement with the trend in instrumental data.

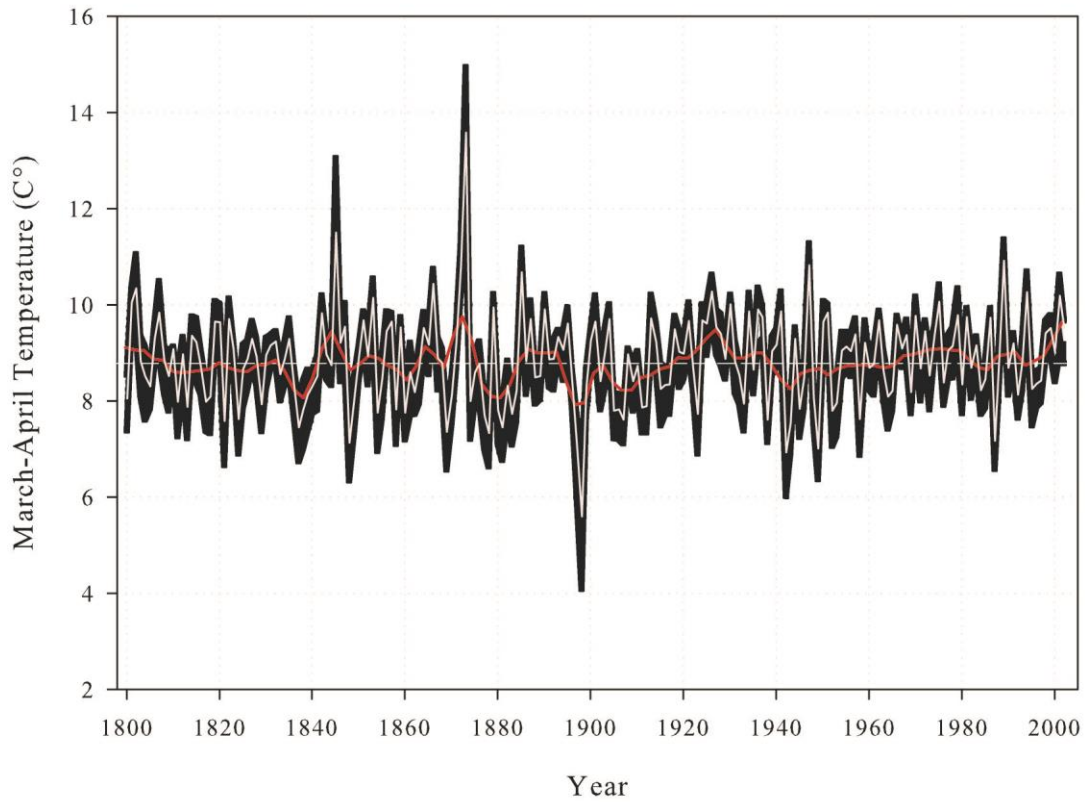


Figure 6. March–April temperature reconstruction for Turkey for the period 1800–2002 CE. The central horizontal line (dashed white) shows the reconstructed long-term mean and does not include instrumental data; black background denotes Monte Carlo ($n = 1000$) bootstrapped 95% confidence limits; and the red line shows 13-year low-pass filter values.

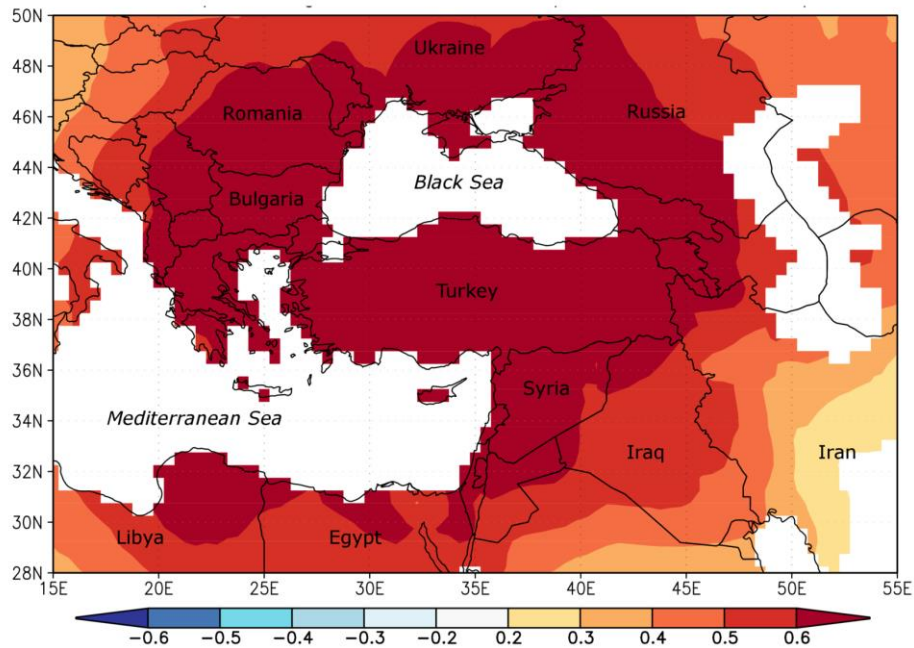


Figure 7. Spatial correlation map for the March–April temperature reconstruction. Spatial field correlation map showing statistical relationship between the temperature reconstruction and the gridded temperature field at 0.5° intervals (CRU TS3.23; Jones and Harris 2008) during the period 1930–2002 over the Mediterranean region. For each grid, calculated correlation coefficient from 0.20 to 0.60 is significant ($p < 0.05$).

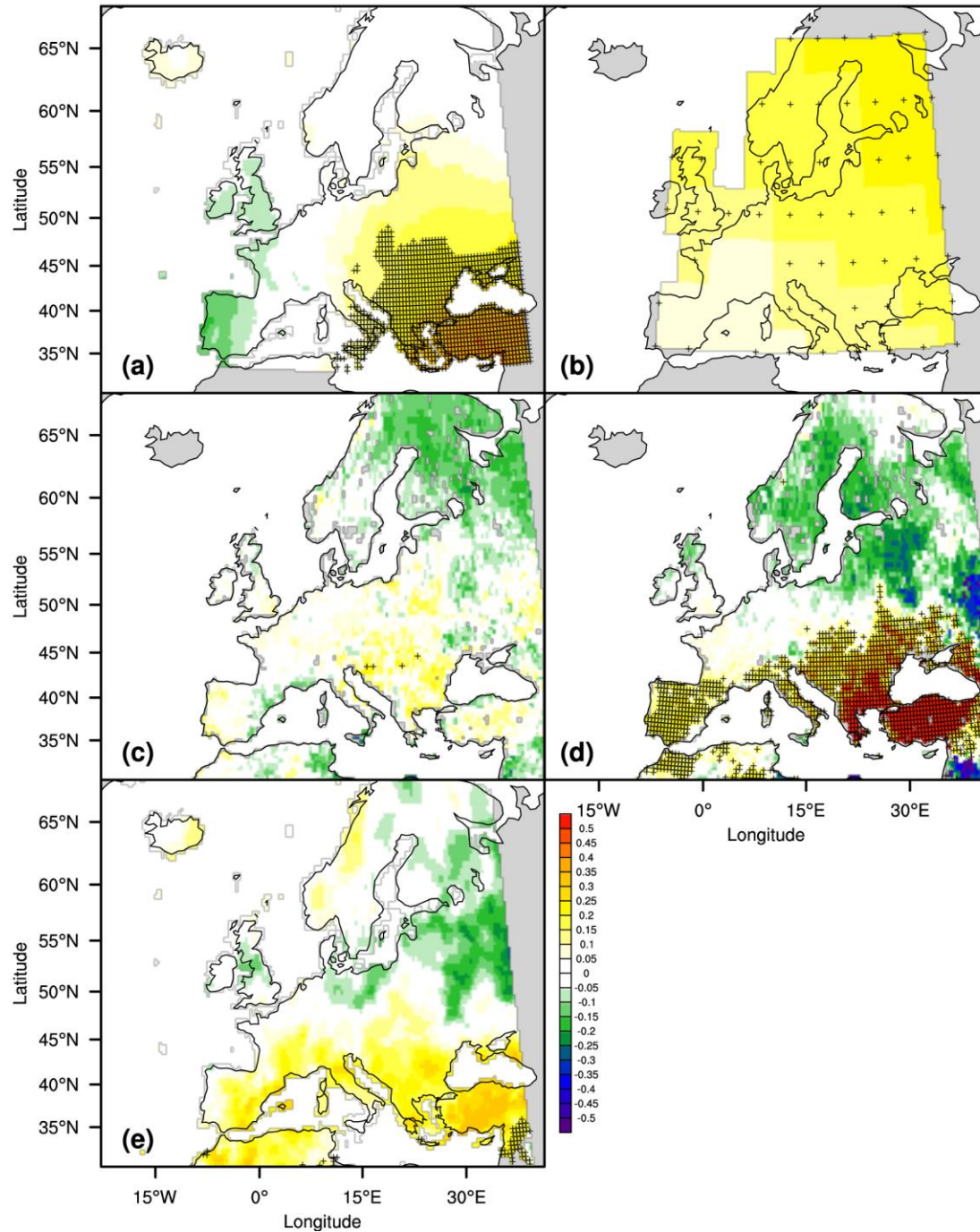


Figure 8. Spatial correlation maps for the March–April temperature reconstruction and precipitation signal (PC1) obtained from tree-ring data set during the period 1800–2002 over Europe. Maps demonstrate spatial field correlations between our temperature reconstruction and (a) gridded spring temperature reconstruction for Europe (Xoplaki et al. 2005), (b) gridded

summer temperature reconstruction for Europe (Luterbacher et al. 2016), (c) Old World Drought Atlas (OWDA; Cook et al. 2015). Panels (d) and (e) show spatial correlations between PC1 and OWDA (Cook et al. 2015) and gridded European summer precipitation reconstruction (Pauling et al., 2006), respectively. ‘+’ represents significant correlation coefficients ($p < 0.05$).

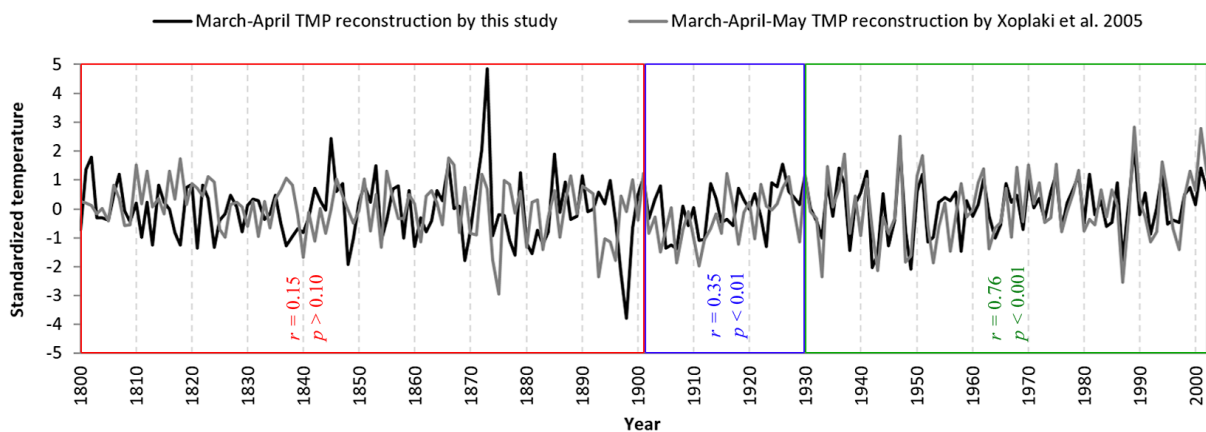


Figure 9. Comparison of March-April temperature reconstruction (gray) with the mean of corresponding grid points from European spring (March to May) temperature reconstruction (Xoplaki et al. 2005; black) over the study area (36–42° N, 26–38° E). The indicated correlation coefficients are calculated for instrumental period (also calibration period for this study) (1930–2002; $r = 0.76$, $p < 0.001$); for the pre-instrumental period of Turkey, while instrumental data has sufficient quality for most part of Europe (1901–1929; $r = 0.35$, $p < 0.10$); and for pre-instrumental period (1800–1900; $r = 0.13$, $p < 0.10$).

**Spring temperature variability over Turkey since 1800 CE reconstructed
from a broad network of tree-ring data**

Nesibe Köse^{(1),*}, H. Tuncay Güner⁽¹⁾, Grant L. Harley⁽²⁾, Joel Guiot⁽³⁾

⁽¹⁾Istanbul University, Faculty of Forestry, Forest Botany Department 34473 Bahçeköy-Istanbul,
Turkey

⁽²⁾University of Southern Mississippi, Department of Geography and Geology, 118 College
Drive Box 5051, Hattiesburg, Mississippi, 39406, USA

⁽³⁾Aix-Marseille Université, CNRS, IRD, CEREGE UM34, ECCOREV, 13545 Aix-en-
Provence, France

*Corresponding author. Fax: +90 212 226 11 13
E-mail address: nesibe@istanbul.edu.tr

20 **Abstract**

21 The meteorological observational period in Turkey, which starts *ca.* 1930 CE, is too short for
22 understanding long-term climatic variability. Tree rings have been used intensively as proxy
23 records to understand summer precipitation history of the region, primarily because of having a
24 dominant precipitation signal. Yet,, the historical context of temperature variability is unclear.
25 Here we used higher order principle components of a network of 23 tree-ring chronologies to
26 provide a high-resolution spring (March–April) temperature reconstruction over Turkey during
27 the period 1800–2002. The reconstruction model accounted for 67% ($\text{Adj. } R^2 = 0.64, p < 0.0001$)
28 of the instrumental temperature variance over the full calibration period (1930–2002). The
29 reconstruction is punctuated by a temperature increase during the 20th century; yet extreme cold
30 and warm events during the 19th century seem to eclipse conditions during the 20th century.. We
31 found significant correlations between our March–April spring temperature reconstruction and
32 existing gridded spring temperature reconstructions for Europe over Turkey and southeastern
33 Europe. Moreover, the precipitation signal obtained from the tree-ring network (first principle
34 component) showed highly significant correlations with gridded summer drought index
35 reconstruction over Turkey and Mediterranean countries. Our results showed that, beside the
36 dominant precipitation signal, a temperature signal can be extracted from tree-ring series and
37 they can be useful proxies to reconstruct past temperature variability.

38

39 KEYWORDS: Dendroclimatology, Climate reconstruction, *Pinus nigra*, Principle component
40 analysis, Spring temperature.

41 1 Introduction

42

43 Long term meteorological observations in the Mediterranean region allow access to 100 years of
44 instrumental recordings of temperature, precipitation and pressure in most of the region.
45 Moreover, natural archives as well as documentary information provide resources with which to
46 make sensitive climate reconstructions. An extensive body of literature details climate changes

47 in the Mediterranean region over the last two millennia (~~cf. Lionello, P. (Ed.)~~ Luterbacher et al.,
48 2012). Paleolimnological studies provide evidence that the Medieval Climatic Anomaly (MCA;
49 900–1300 CE) characterized warm and dry conditions over the Iberian Peninsula, while the Little
50 Ice Age (LIA; 1300–1850 CE) brought opposite climate conditions, forced by interactions
51 between the East Atlantic and North Atlantic Oscillation (Sanchez-Lopez et al. 2016). In
52 addition, Roberts et al. (2012) highlighted an intriguing spatial dipole NAO pattern between the
53 western and eastern Mediterranean region, which brought anti-phased warm (cool) and wet (dry)
54 conditions during the MCA and LIA. The hydro-climate patterns revealed by previous
55 investigations appear to have been forced not only by NAO, but other climate modes with non-
56 stationary teleconnections across the region (Roberts et al. 2012).

57

58 The climate of Turkey is mainly characterized by Mediterranean macro climate (Türkeş, 1996a).
59 Contrary to the most countries in the Mediterranean region, Turkey has relatively short
60 meteorological records, which start in the 1930s, for understanding long-term climatic
61 variability. On the other hand, proxy records such as speleothems (Fleitmann et al. 2009, Jex et
62 al. 2010, Göktürk et al. 2011), lake sediments (Wick et al. 2003, Jones et al. 2006, Roberts et al.
63 2008, 2012, Kuzucuoğlu et al. 2011, Woodbridge and Roberts 2011, Ülgen et al. 2012, Dean et

Biçimlendirilmiş: İki Yana Yasla

Biçimlendirilmiş: Yazı tipi: İtalik Değil

Biçimlendirilmiş: İki Yana Yasla

64 al. 2013) and tree-rings, have been used to reconstruct long term hydroclimate conditions over
65 Turkey. Tree rings in particular have shown to provide useful information about the past climate
66 of Turkey and were used intensively during the last decade to reconstruct precipitation in the
67 Aegean (Griggs et al. 2007), Black Sea (Akkemik et al. 2005, 2008; Martin-Benitto et al. 2016),
68 Mediterranean regions (Touchan et al. 2005a), as well as the Sivas (D'Arrigo & Cullen 2001),
69 southwestern (Touchan et al. 2003, Touchan et al. 2007; Köse et al. 2013), south-central
70 (Akkemik & Aras 2005) and western Anatolian (Köse et al. 2011) regions of Turkey. These
71 studies used tree rings to reconstruct precipitation because available moisture is often found to be
72 the most important limiting factor that influences radial growth of many tree species in Turkey.
73 These studies revealed past spring-summer precipitation, and described past dry and wet events
74 and their duration. Recently, Cook et al. (2015) presented Old World Drought Atlas (OWDA),
75 which is a set of year by year maps of reconstructed Palmer Drought Severity Index from tree-
76 ring chronologies over the Europe and Mediterranean Basin.

77
78 Besides detailed information on precipitation history represented by these paleoscientific studies,
79 we have still very limited knowledge of past temperature variability of Turkey. For example,
80 significant decreases in spring diurnal temperature ranges (DTR) occurred throughout Turkey
81 from 1929 to 1999 (Turkes & Sumer 2004). This decrease in spring DTRs was characterized by
82 day-time temperatures that remained relatively constant while a significant increase in night-time
83 temperatures were recorded over western Turkey and were concentrated around urbanized and
84 rapidly-urbanizing cities. The historical context of this gradual warming trend in spring
85 temperatures is unclear. Heinrich et al. (2013) provided a winter-to-spring temperature proxy for
86 Turkey from carbon isotopes within the growth rings of *Juniperus excelsa* M. Bieb. since AD

87 1125. Low-frequency temperature trends corresponding to the end of Medieval Climatic
88 Anomaly and Little Ice Age were identified in the record, but the proxy failed to identify the
89 recent warming trend during the 20th century. In this study, we present a tree-ring based spring
90 temperature reconstruction from Turkey and compare our results to previous reconstructions of
91 temperature and precipitation to provide a more comprehensive understanding of climate
92 conditions during the 19th and 20th centuries.

93

94 **2 Data and Methods**

95 2.1 Climate of the Study Area

96

97 The study area, which spans 36–42° N and 26–38° E, was based on the distribution of available
98 tree-ring chronologies. This vast area covers much of western Anatolia and includes the western
99 Black Sea, Marmara, and western Mediterranean regions. Much of this area is characterized by a
100 Mediterranean climate that is primarily controlled by polar and tropical air masses (Türkeş
101 1996a, Deniz et al. 2011). In winter, polar fronts from the Balkan Peninsula bring cold air that is
102 centered in the Mediterranean. Conversely, the dry, warm conditions in summer are dominated
103 by weak frontal systems and maritime effects. Moreover, the Azores high-pressure system in
104 summer and anticyclonic activity from the Siberian high-pressure system often cause below
105 normal precipitation and dry sub-humid conditions over the region (Türkeş 1999, Deniz et al.
106 2011). In this Mediterranean climate, annual mean temperature and precipitation range from 3.6
107 °C to 20.1 °C and from 295 to 2220 mm, respectively, both of which are strongly controlled by
108 elevation (Deniz et al. 2011).

109

2.2 Development of tree-ring chronologies

To investigate past temperature conditions, we used a network of 23 tree-ring site chronologies (Fig. 1). Fifteen chronologies were produced by previous investigations (Mutlu et al. 2011, Akkemik et al. 2008, Köse et al. unpublished data, Köse et al. 2011, Köse et al. 2005) that focused on reconstructing precipitation in the study area. In addition, we sampled eight new study sites and developed tree-ring time series for these areas (Table 1). Increment cores were taken from living *Pinus nigra* Arnold and *Pinus sylvestris* L. trees and cross-sections were taken from *Abies nordmanniana* (Steven) Spach and *Picea orientalis* (L.) Link trunks.

Samples were processed using standard dendrochronological techniques (Stokes & Smiley 1968, Orvis & Grissino-Mayer 2002, Speer 2010). Tree-ring widths were measured, then visually crossdated using the list method (Yamaguchi 1991). We used the computer program COFECHA, which uses segmented time-series correlation techniques, to statistically confirm our visual crossdating (Holmes 1983, Grissino-Mayer 2001). Crossdated tree-ring time series were then standardized by fitting a 67% cubic smoothing spline with a 50% cutoff frequency to remove non-climatic trends related to the age, size, and the effects of stand dynamics using the ARSTAN program (Cook 1985, Cook et al. 1990a). These detrended series were then pre-whitened with low-order autoregressive models to produce time series with a strong common signal and without biological persistence. These series may be more suitable to understand the effect of climate on tree-growth, even if any persistence due to climate might be removed by pre-whitening. For each chronology, the individual series were averaged to a single chronology by

132 computing the biweight robust means to reduce the influences of outliers (Cook et al. 1990b). In
133 this research we used residual chronologies obtained from ARSTAN to reconstruct temperature.
134
135 The mean sensitivity, which is a metric representing the year-to-year variation in ring width
136 (Fritts 1976), was calculated for each chronology and compared. The minimum sample depth for
137 each chronology was determined according to expressed population signal (EPS), which we used
138 as a guide for assessing the likely loss of reconstruction accuracy. Although arbitrary, we
139 required the commonly considered threshold of $EPS > 0.85$ (Wigley et al. 1984; Briffa & Jones
140 1990).

141

142 2.3 Identifying relationship between tree-ring width and climate

143

144 We extracted high resolution monthly temperature and precipitation records from the climate
145 dataset CRU TS 3.23 gridded at 0.5° intervals (Jones and Harris 2008) from KNMI Climate
146 Explorer (<http://climexp.knmi.nl>) for $36\text{--}42^\circ\text{N}$, $26\text{--}38^\circ\text{E}$. The period AD 1930–2002 was
147 chosen for the analysis because it maximized the number of station records within the study area.

148

149 First, the climate-growth relationships were investigated with response function analysis (RFA)
150 (Fritts 1976) for biological year from previous October to current October using the
151 DENDROCLIM2002 program (Biondi & Waikul 2004). This analysis is done to determine the
152 months during which the tree-growth is the most responsive to temperature. RFA results showed
153 that precipitation from May to August and temperature in March and April have dominant
154 control on tree-ring formation in the area. Second, we produced correlation maps showing

155 correlation coefficients between tree-ring chronologies and the climate factors most important
156 for tree growth, which are May–August precipitation and March–April temperature, to find the
157 spatial structure of radial growth-climate relationship (St. George 2014, St. George and Ault
158 2014, Hellmann et al. 2016). For each site we used the closest gridded temperature and
159 precipitation values.

160

161 2.4 Temperature reconstruction

162

163 The climate reconstruction is performed by regression based on the principal component (PCs)
164 of the 23 chronologies within the study area. Principle Component Analysis (PCA) was done
165 over the entire period in common to the tree-ring chronologies. The significant PCs were
166 selected by stepwise regression. We combined forward selection with backward elimination
167 setting $p < 0.05$ as entrance tolerance and $p < 0.10$ as exit tolerance. The final model obtained
168 when the regression reaches a local minimum of the root mean squared error (RMSE). The order
169 of entry of the PCs into the model was PC₃, PC₂₁, PC₄, PC₁₅, PC₅, PC₁₇, PC₇, PC₉, PC₁₀. The
170 regression equation is calibrated on the common period (1930–2002) between robust temperature
171 time-series and the selected tree-ring series. Third, the final reconstruction is based on bootstrap
172 regression (Till and Guiot 1990), a method designed to calculate appropriate confidence intervals
173 for reconstructed values and explained variance even in cases of short time-series. It consists in
174 randomly resampling the calibration datasets to produce 1000 calibration equations based on a
175 number of slightly different datasets.

176

177 The quality of the reconstruction is assessed by a number of standard statistics. The overall
178 quality of fit of reconstruction is evaluated based on the determination coefficient (R^2), which
179 expresses the percentage of variance explained by the model and RMSE, which expresses the
180 calibration error. This does not insure the quality of the extrapolation which needs additional
181 statistics based on independent observations, i.e. observations not used by the calibration
182 (verification data). They are provided by the observations not resampled by the bootstrap
183 process. The prediction RMSE (called RMSEP), the reduction of error (RE) and the coefficient
184 of efficiency (CE) are calculated on the verification data and enable to test the predictive quality
185 of the calibrated equations (Cook et al. 1994). Traditionally, a positive RE or CE values means a
186 statistically significant reconstruction model, but bootstrap has the advantage to produce
187 confidence intervals for such statistics without theoretical probability distribution and finally we
188 accept the RE and CE for which the lower confidence margin at 95% are positive. This is more
189 constraining than just accepting all positive RE and CE. For additional verification, we also
190 present traditional split-sample procedure results that divided the full period into two subsets of
191 equal length (Meko and Graybill 1995).

192
193 To identify the extreme March–April cold and warm events in the reconstruction, standard
194 deviation (SD) values were used. Years one and two SD above and below the mean were
195 identified as warm, very warm, cold, and very cold years, respectively. As a way to assess the
196 spatial representation of our temperature reconstruction, we conducted a spatial field correlation
197 analysis between reconstructed values and the gridded CRU TS3.23 temperature field (Jones and
198 Harris 2008) for a broad region of the Mediterranean over the entire instrumental period (ca.
199 1930–2002). Finally, we compared our temperature reconstruction and also precipitation signal

(PC1) against existing gridded temperature and hydroclimate reconstructions for Europe over the period 1800–2002. We performed spatial correlation analysis between [1] our temperature reconstruction and gridded temperature reconstructions for Europe (Xoplaki et al. 2005, Luterbacher et al. 2016) and OWDA (Cook et al. 2015); and [2] PC1 and summer precipitation reconstruction (Pauling et al., 2006) and Old World Drought Atlas (OWDA) (Cook et al. 2015).

To assess the significance of the correlation between our reconstruction (y) and gridded reconstructions (x_j , $j=1 \dots N$), we have calculated significance thresholds based on a Monte-Carlo technique. For each gridpoint j , we have calculated the correlation between x_j and y , but with a random permutation of the values of our reconstruction. This is repeated 1000 times with a different permutation. The 1000 correlation coefficients so obtained are expected to be zero as the correlation is established on non corresponding years. The 95th quantile of these 1000 coefficients is assumed to be passed in less than 5% of the cases. Then a correlation coefficient with a higher value is considered as positive with a 95% confidence. These thresholds are obtained with a common permutation for all x_j so that the spatial structure is conserved in the tests. The sign + is assigned to the x_j with a correlation higher than an expected value under the non-correlation hypothesis.

2 Results and Discussion

2.1 Tree-ring chronologies

In addition to 15 chronologies developed by previous studies, we produced six *P. nigra*, one *P. sylvestris*, one *A. nordmanniana* / *P. orientalis* chronologies for this study (Table 2). The Çorum district produced two *P. nigra* chronologies: one the longest (KAR; 627 years long) and the other the most sensitive to climate (SAH; mean sensitivity value of 0.25). Previous investigations of

climate-tree growth relationships reported a mean sensitivity range of 0.13–0.25 for *P. nigra* in Turkey (Köse 2011, Akkemik et al. 2008). The KAR, SAH, and ERC chronologies (with mean sensitivity values from 0.22 to 0.25) were classified as very sensitive, and the SAV, HCR, and PAY chronologies (mean sensitivity values range 0.17–0.18) contained values characteristic of being sensitive to climate. The lowest mean sensitivity value was obtained for the ART A. *nordmanniana* / *P. orientalis* chronology. Nonetheless, this chronology retained a statistically significant temperature signal ($p < 0.05$).

230

2.2 Tree-ring growth-climate relationship

RFA coefficients of May to August precipitation are positively correlated with most of the tree-ring series (Fig. 2) and among them, May and June coefficients are generally significant. The first principal component of the 23 chronologies, which explains 47% of the tree-growth variance, is highly correlated with May–August total precipitation, statistically ($r = 0.65$, $p < 0.001$) and visually (Fig. 3). The high correlation was expected given that numerous studies also found similar results in Turkey (Akkemik 2000a, Akkemik 2000b, Akkemik 2003, Akkemik et al. 2005, Akkemik et al. 2008, Akkemik & Aras 2005, Hughes et al. 2001, D’Arrigo & Cullen 2001, Touchan et al. 2003; Touchan et al. 2005a, Touchan et al. 2005b, Touchan et al. 2007, Köse et al. 2011, Köse et al. 2012, Köse et al. 2013, Martin-Benitto et al. 2016). The influence of temperature was not as strong as May–August precipitation on radial growth, although generally positive in early spring (March and April) (Fig. 2). Conversely, the ART chronology from northeastern Turkey contained a strong temperature signal, which was significantly positive in March.

Correlation maps representing influence of May-August precipitation (Fig. 4a) and March-April temperature (Fig 4b) also showed that strength of the summer precipitation signal is higher and significant almost all over the Turkey. Higher precipitation in summer has a positive effect on tree-growth, because of long-lasting dry and warm conditions over the Turkey (Türkeş 1996b, Köse et al. 2012). Spring precipitation signal are generally positive and significant only for four tree-ring sites. The sites located at the upper distributions of the species are generally showed higher correlations. The highest correlations obtained for *Picea/Abies* chronology (ART) from the Caucasus, and for *Pinus nigra* chronology (HCR) from the upper (about 1900 m) and southeastern distribution of the species. This black pine forest was still partly covered by snow from previous year during the field work in fall. Higher temperatures in spring maybe cause snow melt earlier and lead to produce larger annual rings. In addition to these chronologies, we also used the chronologies that revealed the influence of precipitation, as well as temperature to reconstruct March–April temperature.

258

259

2.3 March-April temperature reconstruction

The higher order PCs of the 23 chronologies are significantly correlated with the March–April temperature and, by nature, are independent on the precipitation signal (Table 3). The best selection for fit temperature are obtained with the PC₃, PC₄, PC₅, PC₇, PC₉, PC₁₀, PC₁₅, PC₁₇, PC₂₁, which explains together 25% of the tree-ring chronologies. So the temperature signal remains important in the tree-ring chronologies and can be reconstructed. The advantage to separate both signals through orthogonal PCs enable to remove an unwanted noise for our temperature reconstruction. Thus, PC₁ was not used as potential predictor of temperature because

268 it is largely dominated by precipitation (Table 3, Fig. 3). The last two PCs contain a too small
269 part of the total variance to be used in the regressions. However, even if Jolliffe (1982) and Hadi
270 & Ling (1998) claimed that certain PCs with small eigenvalues (even the last one), which are
271 commonly ignored by principal components regression methodology, may be related to the
272 independent variable, we must be cautious with that because they may be much more dominated
273 by noise than the first ones. So, the contribution of each PC to the regression sum of squares is
274 also important for selection of PCs (Hadi & Ling 1998). The findings of Jolliffe (1982) and Hadi
275 & Ling (1998) provide a justification for using non-primary PCs, (*e.g.*, of second and higher
276 order) in our regression, given that correlations with temperature may be over-powered by
277 affects from precipitation in our study area (Cook 2011, personal communication).

278
279 Using this method, the calibration and verification statistics indicated a statistically significant
280 reconstruction (Table 4, Fig. 5). For additional verification, we also present split-sample
281 procedure results. Similarly bootstrap results, the derived calibration and verification tests using
282 this method indicated a statistically significant RE and CE values (Table 5).

283
284 The regression model accounted for 67% ($\text{Adj. } R^2 = 0.64, p < 0.0001$) of the actual temperature
285 variance over the calibration period (1930–2002). Also, actual and reconstructed March–April
286 temperature values had nearly identical trends during the period 1930–2002 (Fig. 5). Moreover,
287 the tree-ring chronologies successfully simulated both high frequency and warming trends in the
288 temperature data during this period. The reconstruction was more powerful at classifying warm
289 events rather than cold events. Over the last 73 years, eight of ten warm events in the
290 instrumental data were also observed in the reconstruction, while five of nine cold events were

291 captured. Similarly, previous tree-ring based precipitation reconstructions for Turkey (Köse et al.
292 2011; Akkemik et al. 2008) were generally more successful in capturing dry years rather than
293 wet years.

294

295 Our temperature reconstruction on the 1800–2002 period is obtained by bootstrap regression,
296 using 1000 iterations (Fig. 6). The confidence intervals are obtained from the range between the

297 2.5th and the 97.5th percentiles of the 1000 simulations. Low frequency variability of our spring
298 temperature reconstruction showed larger variability in nineteenth century than twentieth
299 century. For the pre-instrumental period (1800–1929), a total of 23 cold (1813, 1818, 1821,

300 1824, 1837, 1848, 1854, 1858, 1860, 1869, 1877–1878, 1880–1881, 1883, 1897–1898, 1905–
301 1907, 1911–1912, 1923) and 13 warm (1801–1802, 1807, 1845, 1853, 1866, 1872–1873, 1879,
302 1885, 1890, 1901, 1926) events were determined. After comparing our results with event years
303 obtained from May–June precipitation reconstructions from western Anatolia (Köse et al. 2011),
304 the cold years 1818, 1848, and 1897 appeared to coincide with wet years and 1881 was a very
305 wet year for the entire region. Furthermore, these years can be described as cold (in March–
306 April) and wet (in May–June) for western Anatolia.

307

308 Among the warm periods in our reconstruction, conditions during the year 1879 were dry, 1895
309 wet, and 1901 very wet across the broad region of western Anatolia (Köse et al. 2011). Hence,
310 we defined 1879 as a warm (in March–April) and dry year (in May–June), and 1895 and 1901
311 were warm and wet years. In the years 1895 and 1901 the combination of a warm early spring
312 and a wet late spring-summer caused enhanced radial growth in Turkey, interpreted as longer
313 growing seasons without drought stress.

314

315 Of these event years, 1897 and 1898 were exceptionally cold and 1845, 1872 and 1873 were
316 exceptionally warm. During the last 200 years, our reconstruction suggests that the coldest year
317 was 1898 and the warmest year was 1873. The reconstructed extreme events also coincided with
318 accounts from historical records. Server (2008) recounted the winter of 1898 as characterized by
319 anomalously cold temperatures that persisted late into the spring season. A family, who brought
320 their livestock herds up into the plateau region in Kırşehir seeking food and water were suddenly
321 covered in snow on 11 March 1898. This account of a late spring freeze supports the
322 reconstruction record of spring temperatures across Turkey, and offers corroboration to the
323 quality of the reconstructed values.

324

325 Seyf (1985) reported that extreme summer temperature during the year 1873 resulted in
326 widespread crop failure and famine. Historical documents recorded an infamous drought-derived
327 famine that occurred in Anatolia from 1873 to 1874 (Quataert, 1996, Kuniholm, 1990), which
328 claimed the lives of 250,000 people and a large number of cattle and sheep (Faroghi, 2009). This
329 drought caused widespread mortality of livestock and depopulation of rural areas through human
330 mortality, and migration of people from rural to urban areas. Further, the German traveler
331 Naumann (1893) reported a very dry and hot summer in Turkey during the year 1873 (Heinrich
332 et al, 2013). Conditions worsened when the international stock exchanges crashed in 1873
333 (Zürcher, 2004). Our temperature record suggests that dry conditions during the early 1870s
334 were possibly exacerbated by warm spring temperatures that likely carried into summer. A
335 similar pattern of intensified drought by warm temperatures was demonstrated recently by
336 Griffin and Anchukaitis (2014) for the current drought in California, USA.

337
338 Extreme cold and warm events were usually one year long, and the longest extreme cold and
339 warm events were two and three years, respectively. These results were similar with durations of
340 extreme wet and dry events in Turkey (Touchan et al. 2003, Touchan et al. 2005a, Touchan et al.
341 2005b, Touchan et al. 2007, Akkemik & Aras, 2005, Akkemik et al. 2005, Akkemik et al. 2008,
342 Köse et al. 2011, Güner et al. 2016). Moreover, seemingly innocuous short-term warm events,
343 such as the 1807 event, were recorded across the Mediterranean and in high elevations of the
344 European regions. Casty et al. (2005) reported the year 1807 as being one of the warmest alpine
345 summers in the European Alps over the last 500 years. As such, a drought record from Nicault et
346 al. (2008) echoes this finding, as a broad region of the Mediterranean basin experienced drought
347 conditions.

348
349 ~~Low frequency variability of our spring temperature reconstruction showed larger variability in~~
350 ~~nineteenth century than twentieth century. Similar results observed on previous tree-ring based~~
351 ~~precipitation reconstructions from Turkey (Touchan et al. 2003, D'Arrigo et al. 2001, Akkemik~~
352 ~~and Aras 2005, Akkemik et al. 2005, Köse et al. 2011). Moreover, cold (warm) periods observed~~
353 ~~in our reconstruction are generally appeared as generally wet in the precipitation reconstructions,~~
354 ~~while rarely correlated with dry (wet) periods (Fig. 7). When we compare the relationship~~
355 ~~between temperature and precipitation over the instrumental period, both case, cold (warm) and~~
356 ~~wet (dry) as well as cold (warm) and dry (wet), can be observed.~~

357
358 Heinrich et al. (2013) analyzed winter-to-spring (January–May) air temperature variability in
359 Turkey since AD 1125 as revealed from a robust tree-ring carbon isotope record from *Juniperus*

360 *excelsa*. Although they offered a long-term perspective of temperature over Turkey, the
361 reconstruction model, which covered the period 1949–2006, explained 27% of the variance in
362 temperature since the year 1949. In this study, we provided a short-term perspective of
363 temperature fluctuation based on a robust model (calibrated and verified 1930–2002; Adj. $R^2 =$
364 0.64; $p < 0.0001$). Yet, the Heinrich et al. (2013) temperature record did not capture the 20th
365 century warming trend as found elsewhere (Wahl et al. 2010). However, their temperature trend
366 does agree with trend analyses conducted on meteorological data from Turkey and other areas in
367 the eastern Mediterranean region. The warming trend seen during our reconstruction calibration
368 period (1930–2002) was similar to the data shown by Wahl et al. (2010) across the region and
369 hemisphere. Further, the warming trends seen in our record agrees with data presented by Turkes
370 & Sumer (2004), of which they attributed to increased urbanization in Turkey. Considering long-
371 term changes in spring temperatures, the 19th century was characterized by more high-frequency
372 fluctuations compared to the 20th century, which was defined by more gradual changes and
373 includes the beginning of decreased DTRs in the region (Turkes & Sumer 2004).

374

375 | 4.2.4 Comparison with instrumental gridded data and spatial reconstructions

376

377 Spatial correlation analysis revealed that our network-based temperature reconstruction was
378 representative of conditions across Turkey, as well as the broader Mediterranean region (Fig.
379 | 78). During the period 1930–2002, estimated temperature values were highly significant (r range
380 0.5–0.6, $p < 0.01$) with instrumental conditions recorded from southern Ukraine to the west
381 across Romania, and from northern areas of Libya and Egypt to the east across Iraq. The strength
382 of the reconstruction model is evident in the broad spatial implications demonstrated by the

Biçimlendirilmiş: Yazı tipi: Kalın Değil

383 temperature record. Thus, we interpret warm and cold periods and extreme events within the
 384 record with high confidence.
 385
 386 We compared our tree-ring based temperature reconstruction with existing gridded temperature
 387 reconstructions for Europe (Xoplaki et al. 2005, Luterbacher et al. 2016) and the Old World
 388 Drought Atlas (OWDA) (Cook et al. 2015) for further validation of the reconstruction (Fig. 89a,
 389 b, c, respectively). Spatial correlations over the past 200 years were lower with reconstructed
 390 European summer temperature (May to July) (Fig. 89b). Yet, we expected this result because of
 391 the paucity of Turkey-derived proxies in the other reconstructions, as well as the differing
 392 seasons involved across the reconstructions. Similarly, our reconstruction showed weak
 393 correlations with summer drought index over Turkey. Beside comparing different seasons,
 394 perhaps this is because less precipitation begets drought conditions rather than high temperature
 395 in the region. The highest and significant ($p < 0.05$) correlations were found with European
 396 spring (March to May) temperature reconstruction over southeastern Europe, which are stronger
 397 over Turkey (Fig. 89a). We used the mean of corresponding grid points from European spring
 398 temperature reconstruction over the study area (36–42° N, 26–38° E) to show how the correlation
 399 changed over time (Fig. 949). The correlation coefficient was highly significant ($r = 0.76$, $p <$
 400 0.001) during our calibration period (1930–2002). We found lower but still significant
 401 correlation ($r = 0.35$, $p < 0.10$) for the period of 1901–1929, which climatic records are very few
 402 over the region while available data has sufficient quality for most part of Europe. These results
 403 give additional verification for our reconstruction. Moreover, our reconstruction has a weak,
 404 insignificant relationship ($r = 0.13$, $p > 0.10$) during the 19th century. This may be related to poor
 405 reconstructive skill of European spring temperature reconstruction over Turkey, which contains

few proxies from the country (Xoplaki et al. 2005, Luterbacher et al. 2004). Nonetheless, these results demonstrate that tree-ring chronologies from Turkey can serve as useful temperature proxies for further spatial temperature reconstructions to fill the gaps in the area.

We also compared the precipitation signal (PC1) obtained from our tree-ring network with Old World Drought Atlas (OWDA) (Cook et al. 2015) and gridded European summer precipitation reconstruction (Pauling et al., 2006) to test the strength of the signal spatially (Fig. 89d and e, respectively). We calculated highly significant positive correlations with summer drought index over Turkey and neighboring European countries such as Greece, Bulgaria, and Romania, Italy while significant correlations are lower for the other-northern Mediterranean countries (Fig. 89d). These results showed that summer precipitation signal represented by PC1 is very strong not only on instrumental period, but also on pre-instrumental period, and represents a large spatial coverage. We found lower but still and in-significant correlations over Turkey and Mediterranean countries with European summer precipitation reconstruction (Fig. 89e). Pauling et al. (2006) stated that poor reconstructive skills determined over Turkey because of few instrumental record before the 1930s. ~~These results showed that summer precipitation signal represented by PC1 is very strong not only on instrumental period, but also on pre-instrumental period, and represents a large spatial coverage.~~

4 Conclusions

In this study, we used a broad network of tree-ring chronologies to provide the first tree-ring based temperature reconstruction for Turkey and identified extreme cold and warm events during

429 the period 1800–1929 CE. Similar to the precipitation reconstructions against which we compare
430 our air temperature record, extreme cold and warm years were generally short in duration (one
431 year) and rarely exceeded two-three years in duration. The coldest and warmest years over
432 western Anatolia were experienced during the 19th century, and the 20th century is marked by a
433 temperature increase.

434
435 Reconstructed temperatures for the 19th century suggest that more short-term fluctuations
436 occurred compared to the 20th century. The gradual warming trend shown by our reconstruction
437 calibration period (1930–2002) is coeval with decreases in spring DTRs. Given the results of
438 Turkes and Sumer (2004), the variations in short- and long-term temperature changes between
439 the 19th and 20th centuries might be related to increased urbanization in Turkey.

440
441 We highlight that the 20th century warming trend is unprecedented within the context of the past
442 *ca.* 200 years, especially over the past *ca.* 15 years. Correlations with gridded climate fields and
443 other climate reconstructions from the region revealed that our network-based temperature
444 reconstruction was representative of conditions across Turkey, as well as the broader
445 Mediterranean region. Expanding the tree-ring network across Turkey, especially to the east, will
446 improve the spatial implications of future temperature reconstructions.

447
448 The study revealed the potential for reconstructing temperature in an area previously thought
449 impossible, especially given the strong precipitation signals displayed by most tree species
450 growing in the dry Mediterranean climate that characterizes broad areas of Turkey. Our
451 reconstruction only spans 205 years due to the shortness of the common interval for the

452 chronologies used in this study, but the possibility exists to extend our temperature
453 reconstruction further back in time by increasing the sample depth with more temperature-
454 sensitive trees, especially from northeastern Turkey. Thus future research will focus on
455 increasing the number of tree-ring sites across Turkey, and maximizing chronology length at
456 existing sites that would ultimately extend the reconstruction back in time.

457

458 **Acknowledgements**

459

460 This research was supported by The Scientific and Technical Research Council of Turkey
461 (TUBITAK); Projects ÇAYDAG 107Y267 and YDABAG 102Y063. N. Köse was supported by
462 The Council of Higher Education of Turkey. We are grateful to the Turkish Forest Service
463 personnel and Ali Kaya, Umut Ç. Kahraman and Hüseyin Yurtseven for their invaluable support
464 during our field studies. We thank to Dr. Ufuk Turuncoğlu for his help on spatial analysis. J.
465 Guiot was supported by the Labex OT-Med (ANR-11-LABEX-0061), French National Research
466 Agency (ANR).

467

468 **References**

- 469 |
- 470 Akkemik, Ü.: Dendroclimatology of Umbrella pine (*Pinus pinea* L.) in Istanbul (Turkey), Tree-
 471 Ring Bull., 56, 17–20, 2000a.
- 472 Akkemik, Ü.: Tree-ring chronology of *Abies cilicica* Carr. in the Western Mediterranean Region
 473 of Turkey and its response to climate, Dendrochronologia, 18, 73–81, 2000b.
- 474 Akkemik, Ü.: Tree-rings of *Cedrus libani* A. Rich the northern boundary of its natural
 475 distribution, IAWA J, 24(1), 63-73, 2003.
- 476 Akkemik, Ü. and Aras, A.: Reconstruction (1689–1994) of April–August precipitation in
 477 southwestern part of central Turkey, Int. J. Clim., 25, 537–548, 2005.
- 478 Akkemik, Ü., Dagdeviren, N., and Aras, A.: A preliminary reconstruction (A.D. 1635–2000) of
 479 spring precipitation using oak tree rings in the western Black Sea region of Turkey, Int. J.
 480 Biomet., 49(5), 297–302, 2005.
- 481 Akkemik, Ü., D’Arrigo, R., Cherubini, P., Köse, N., and Jacoby, G.: Tree-ring reconstructions of
 482 precipitation and streamflow for north-western Turkey, Int. J. Clim., 28, 173–183, 2008.
- 483 Biondi, F. and Waikul, K.: DENDROCLIM2002: A C++ program for statistical calibration of
 484 climate signals in tree-ring chronologies, Comp. Geosci., 30, 303–311, 2004.
- 485 Briffa, K. R. and Jones, P. D.: Basic chronology statistics and assessment. In: Methods of
 486 Dendrochronology: Applications in the Environmental Sciences (Cook, E. and Kairiukstis, L.
 487 A. eds). Kluwer Academic Publishers, Amsterdam, pp. 137–152, 1990.

488 Casty, C., Wanner, H., Luterbacher, J., Esper, J., and Böhm, R.: Temperature and precipitation
 489 variability in the European Alps since 1500, *Int. J. Clim.*, 25(14), 1855–1880, 2005.

490 Cook, E.: A time series analysis approach to tree-ring standardization. PhD. Dissertation.
 491 University of Arizona, Tucson, 1985.

492 Cook, E., Briffa, K., Shiyatov, S., and Mazepa, V.: Tree-ring standardization and growth-trend
 493 estimation. In: *Methods of Dendrochronology: Applications in the Environmental Sciences*
 494 (Cook, E. and Kairiukstis, L. A. eds). Kluwer Academic Publishers, Amsterdam, pp.104–
 495 122, 1990a.

496 Cook, E., Shiyatov, S., and Mazepa, V.: Estimation of the mean chronology. In: *Methods of*
 497 *Dendrochronology: Applications in the Environmental Sciences* (Cook, E. and Kairiukstis, L.
 498 A. eds). Kluwer Academic Publishers, Amsterdam, pp. 123–132, 1990b.

499 Cook, E.R., Seager R., et al.: Old World megadroughts and pluvials during the Common Era. *Sci. Adv.*, 1, e1500561, doi:10.1126/sciadv.1500561, 2015.

501 D’Arrigo, R. and Cullen, H. M.: A 350-year (AD 1628–1980) reconstruction of Turkish
 502 precipitation. *Dendrochronologia*, 19(2), 169–177, 2001.

503 [Dean, R. J., Jones, M. D., et al.: Palaeo-seasonality of the last two millennia reconstructed from](#)
 504 [the oxygen isotope composition of carbonates and diatom silica from Nar Gölü, central](#)
 505 [Turkey, *Quat. Sci. Rev.*, 66, 35-44, 2013.](#)

506 Deniz, A., Toros, T., and Incecik, S.: Spatial variations of climate indices in Turkey, *Int. J.*
 507 *Clim.*, 31, 394-403, 2011.

508 [Fleitmann, D., Cheng, H., et al.: Timing and climatic impact of Greenland interstadials recorded](#)
 509 [in stalagmites from northern Turkey, Geophys. Res. Lett. 36, L19707. doi:](#)
 510 [10.1029/2009gl040050, 2009.](#)
 511 Fritts, H. C.: Tree Rings and Climate. Academic Press, New York, 1976.
 512 [Gokturk, O.M., Fleitmann, D., Badertscher, S., Cheng, H., Edwards, R.L., Tuysuz, O.:](#)
 513 [Climate on the Southern Black Sea coast during the Holocene, Quat. Sci. Rev., 30, 2433–2445,](#)
 514 [2010.](#)
 515 Griggs, C., DeGaetano, A., Kuniholm, P., and Newton, M.: A regional high-frequency
 516 reconstruction of May–June precipitation in the north Aegean from oak tree rings, A.D.
 517 1809–1989, Int. J. Clim., 27, 1075–1089, 2007.
 518 Grissino-Mayer, H. D.: Evaluating crossdating accuracy: A manual and tutorial for the computer
 519 program COFECHA, Tree-Ring Res., 57, 205–221, 2001.
 520 Griffin, D. and Anchukaitis, K. J.: How unusual is the 2012–2014 California drought? Geophys.
 521 Res. Lett., 41(24), 9017–9023, 2014.
 522 Güner, H.T., Köse, N., Harley, G. L.: 200-year reconstruction of Kocasu River (Sakarya River
 523 Basin, Turkey) streamflow derived from a tree-ring network, Int. J. Biometeorol., DOI
 524 10.1007/s00484-016-1223-y, 2016.
 525 Hadi, A. S. and Ling, R. F.: Some cautionary notes on the use of principal components
 526 regression, Amer. Statist., 52(1), 15–19, 1998.
 527 Heinrich, I., Touchan, R., Liñán, I. D., Vos, H., and Helle, G.: Winter-to-spring temperature
 528 dynamics in Turkey derived from tree rings since AD 1125, Clim. Dynam., 41(7–8), 1685–
 529 1701, 2013.

530 Hellmann, L., Agafonov, L., et al.: Diverse growth trends and climate responses across Eurasia's
 531 boreal forest. *Environmental Research Letters*: 11: 074021, doi:10.1088/1748-
 532 9326/11/7/074021.

533 Holmes, R. L.: Computer-assisted quality control in tree-ring data and measurements, *Tree-Ring*
 534 *Bull.*, 43, 69–78, 1983.

535 Hughes, M. K., Kuniholm, P. I., Garfin, G. M., Latini, C., and Eischeid, J.: Aegean tree-ring
 536 signature years explained, *Tree-Ring Res.*, 57(1), 67–73, 2001.

537 Jolliffe, I. T.: A note on the use of principal components in regression, *Appl. Stat.*, 31(3), 300–
 538 303, 1982.

539 [Jex, C.N., Baker, A., et al.: Calibration of speleothem \$\delta^{18}\text{O}\$ with instrumental climate records](#)
 540 [from Turkey, *Global Planet. Change*, 71, 207–217, 2010.](#)

541 [Jones, M.D., Roberts, N., Leng, M.J., Türkeş, M.: A high-resolution late Holocene lake isotope](#)
 542 [record from Turkey and links to North Atlantic and monsoon climate, *Geology*, 34 \(5\), 361–](#)
 543 [364, 2006.](#)

544 Jones, P. D. and Harris, I.: Climatic Research Unit (CRU) time-series datasets of variations in
 545 climate with variations in other phenomena. NCAS British Atmospheric Data Centre, 2008.
 546 <http://catalogue.ceda.ac.uk/uuid/3f8944800cc48e1cbc29a5ee12d8542d>

547 Köse, N., Akkemik, Ü., and Dalfes, H. N.: Anadolu'nun iklim tarihinin son 500 yılı:
 548 Dendroklimatolojik ilk sonuçlar. Türkiye Kuvaterner Sempozyumu-TURQUA-V, 02–03
 549 Haziran 2005, Bildiriler Kitabı, 136–142 (In Turkish), 2005.

550 Köse, N., Akkemik, Ü., Dalfes, H. N., and Özeren, M. S.: Tree-ring reconstructions of May–June
 551 precipitation of western Anatolia, *Quat. Res.*, 75, 438–450, 2011.

552 Köse, N., Akkemik, Ü., Dalfes, H. N., and Özeren, M. S., Tolunay D.: Tree-ring growth of *Pinus*
553 *nigra* Arn. subsp. *pallasiana* under different climate conditions throughout western Anatolia,
554 *Dendrochronologia*, 295-301, 2012.

555 Köse, N., Akkemik, U., Guner, H.T., Dalfes, H.N., Grissino-Mayer, H.D., Ozeren, M.S., Kindap,
556 T.: An improved reconstruction of May– June precipitation using tree-ring data from western
557 Turkey and its links to volcanic eruptions, *Int. J. Biometeorol*, 57(5), 691–701, 2013.

558 Kuzucuoğlu, C., Dörfler, W., Kunesch, S., Goupille, F.: Mid- to late-Holocene climate change in
559 central Turkey: the Tecer Lake record, *Holocene*, 21, 173–188, 2011.

560 ~~Lionello, P. (Ed.):*The Climate of the Mediterranean Region, from the Past to the Future.*~~
561 ~~Elsevier, Amsterdam, Netherlands, 2012.~~

562 Luterbacher, J., Dietrich, D., Xoplaki, E., Grosjean, M., Wanner, H.: European seasonal and
563 annual temperature variability, trends and extremes since 1500. *Science*, 303, 1499–1503,
564 2004.

565 Luterbacher, J., R. García-Herrera, et al.: A review of 2000 years of paleoclimatic evidence in
566 the Mediterranean. In: Lionello, P. (Ed.), *The Climate of the Mediterranean region: from the*
567 past to the future. Elsevier, Amsterdam, The Netherlands, 87-185, 2012.

568 Luterbacher, J., Werner, J.P., et al.: European summer temperatures since Roman times.
569 *Environmental Research Letters*, 11: 024001, doi:10.1088/1748-9326/11/1/024001, 2016.

570 Martin-Benito, D., Ummenhofer C.C., Köse, N., Güner, H.T., Pederson, N.: Tree-ring
571 reconstructed May-June precipitation in the Caucasus since 1752 CE, *Clim. Dyn.*, DOI
572 10.1007/s00382-016-3010-1, 2016.

573 Meko, D. M. and Graybill, D. A.: Tree-ring reconstruction of upper Gila River discharge, *Wat.*
574 *Res. Bull.*, 31, 605–616, 1995.

Biçimlendirilmiş: Sola

575 Mutlu, H., Köse, N., Akkemik, Ü., Aral, D., Kaya, A., Manning, S. W., Pearson, C. L., and
 576 Dalfes, N.: Environmental and climatic signals from stable isotopes in Anatolian tree rings,
 577 Turkey, Reg. Environ. Change, doi: 10.1007/s1011301102732, 2011.

578 Nicault, A., Alleaume, S., Brewer, S., Carrer, M., Nola, P., and Guiot, J.: Mediterranean drought
 579 fluctuation during the last 500 years based on tree-ring data, Clim. Dynam., 31(2–3), 227–
 580 245, 2008.

581 Orvis, K. H. and Grissino-Mayer, H. D.: Standardizing the reporting of abrasive papers used to
 582 surface tree-ring samples, Tree-Ring Res., 58, 47–50, 2002.

583 Pauling, A., Luterbacher, J., Casty, C., Wanner, H.: Five hundred years of gridded high-
 584 resolution precipitation reconstructions over Europe and the connection to large-scale
 585 circulation. Clim. Dynam., 26, 387–405, 2006.

586 [Roberts, N., Jones, M.D., et al.: Stable isotope records of Late Quaternary climate and hydrology](#)
 587 [from Mediterranean lakes: the ISOMED synthesis, Quat. Sci. Rev., 27, 2426–2441, 2008.](#)

588 Roberts, N., Moreno, A., Valero-Garcés, B.L.: Palaeolimnological evidence for an east-west
 589 climate see-saw in the Mediterranean since AD 900. Glob. Planet. Change, 84, 23–34, 2012.

590 Sanchez-López, G. Hernandez, A., Pla-Ribes, et al.: Climate reconstruction for the last two
 591 millennia in central Iberia: The role of East Atlantic (EA), North Atlantic Oscillation (NAO)
 592 and their interplay over the Iberian Peninsula. Quaternary Science Reviews, 149, 135–150,
 593 2016.

594 Server, M.: Evaluation of an oral history text in the context of social memory and traditional
 595 activity, Milli Folklor 77, 61–68 (In Turkish), 2008.

596 Speer, J. H.: Fundamentals of Tree-Ring Research, University of Arizona Press, Tucson, 2010.

597 St. George, S.: An overview of tree-ring width records across the Northern Hemisphere, *Quat.*
 598 *Sci. Rev.*, 95, 132–150, 2014.
 599 St. George, S., and Ault, T. R.: The imprint of climate within northern hemisphere trees, *Quat.*
 600 *Sci. Rev.*, 89, 1–4, 2014.
 601 Stokes, M. A. and Smiley, T. L.: *An Introduction to Tree-ring Dating*, The University of Arizona
 602 Press, Tucson, 1996.
 603 Till, C. and Guiot, J.: Reconstruction of precipitation in Morocco since A D 1100 based on
 604 *Cedrus atlantica* tree-ring widths, *Quat. Res.*, 33, 337–351, 1990.
 605 Touchan, R., Garfin, G. M., Meko, D. M., Funkhouser, G., Erkan, N., Hughes, M. K., and
 606 Wallin, B. S.: Preliminary reconstructions of spring precipitation in southwestern Turkey
 607 from tree-ring width, *Int. J. Clim.*, 23, 157–171, 2003.
 608 Touchan, R., Xoplaki, E., Funkhouser, G., Luterbacher, J., Hughes, M. K., Erkan, N., Akkemik,
 609 Ü., and Stephan, J.: Reconstruction of spring/summer precipitation for the Eastern
 610 Mediterranean from tree-ring widths and its connection to large-scale atmospheric
 611 circulation, *Clim. Dynam.*, 25, 75–98, 2005a.
 612 Touchan, R., Funkhouser, G., Hughes, M. K., and Erkan, N.: Standardized Precipitation Index
 613 reconstructed from Turkish ring widths, *Clim. Change*, 72, 339–353, 2005b.
 614 Touchan, R., Akkemik, Ü., Huges, M. K., and Erkan, N.: May–June precipitation reconstruction
 615 of southwestern Anatolia, Turkey during the last 900 years from tree-rings, *Quat. Res.*, 68,
 616 196–202, 2007.
 617 Turkes, M.: Spatial and temporal analysis of annual rainfall variations in Turkey, *Int. J. Clim.*,
 618 16, 1057–1076, 1996a.

619 Turkes, M.: Meteorological drought in Turkey: a historical perspective, 1930–1993. In: Drought
 620 Network News, International Drought Information Center, University of Nebraska, 8, pp. 17–
 621 21, 1996b.
 622 Turkes, M.: Vulnerability of Turkey to desertification with respect to precipitation and aridity
 623 conditions. Turk. J. Engineer. Environ Sci., 23, 363–380, 1999.
 624 Turkes, M. and Sumer, U. M.: Spatial and temporal patterns of trends variability in diurnal
 625 temperature ranges of Turkey. Theor. Appl. Clim., 77, 195–227, 2004.
 626 Ülgen, U. B., Franz, S. O., Biltekin, D., Çagatay, M. N., Roeser, P. A., Doner, L., Thein, J.:
 627 Climatic and environmental evolution of Lake Iznik (NW Turkey) over the last ~ 4700 years,
 628 Quatern. Int., 274, 88-101, 2012.
 629 Xoplaki, E., Luterbacher J., Paeth H., Dietrich, D., Grosjean, M., Wanner, H.: European spring
 630 and autumn temperature variability and change of extremes over the last half millennium.
 631 Geophys. Res. Lett., 32, L15713, doi:10.1029/2005GL023424.
 632 Wahl, E. R., Anderson, D. M., Bauer, B. A., Buckner, R., Gille, E. P., Gross, W. S., Hartman,
 633 M., and Shah, A.: An archive of high-resolution temperature reconstructions over the past
 634 two millennia, Geochem. Geophys. Geosyst., 11, Q01001, doi:10.1029/2009GC002817,
 635 2010.
 636 Wick, L., Lemcke, G., Sturm, M.: Evidence of Lateglacial and Holocene climatic change and
 637 human impact in eastern Anatolia: high-resolution pollen, charcoal, isotopic and geochemical
 638 records from the laminated sediments of Lake Van, Turkey, Holocene, 13, 665–675, 2003.
 639 Wigley, T. M. L., Briffa, K. R., and Jones, P. D.: On the average value of correlated time series
 640 with applications in dendroclimatology and hydrometeorology, J. Clim. Appl. Met., 23, 201–
 641 213, 1984.

Biçimlendirilmiş: İki Yana Yasla

- 642 | [Woodbridge, J., Roberts, N.: Late Holocene climate of the Eastern Mediterranean inferred from](#)
643 | [diatom analysis of annually-laminated lake sediments, *Quat. Sci. Rev.*, 30, 3381–3392, 2011.](#)
644 | Yamaguchi, D. K.: A simple method for cross-dating increment cores from living trees. *Can. J.*
645 | *For. Res.*, 21, 414–416, 1991.
- 646 | Zücher, E. J.: *Turkey: A modern history*. Oxford Publishing Services, New York, 2004.

647 Table 1. Site information for the new chronologies developed by this study in Turkey.

Site name	Site code	Species	No. trees/ cores	Aspect	Elev. (m)	Lat. (N)	Long. (E)
Çorum, Kargı, Karakise kayalıkları	KAR	<i>Pinus nigra</i>	22 / 38	SW	1522	41°11'	34°28'
Çorum, Kargı, Şahinkayası mevki	SAH	<i>P. nigra</i>	12 / 21	S	1300	41°13'	34°47'
Bilecik, Muratdere	ERC	<i>P. nigra</i>	12 / 25	SE	1240	39°53'	29°50'
Bolu, Yedigöller, Ayıkaya mevki	BOL	<i>P. sylvestris</i>	10 / 20	SW	1702	40°53'	31°40'
Eskişehir, Mihalıççık, Savaş alanı mevki	SAV	<i>P. nigra</i>	10 / 18	S	1558	39°57'	31°12'
Kayseri, Aladağlar milli parkı, Hacer ormanı	HCR	<i>P. nigra</i>	18 / 33	S	1884	37°49'	35°17'
Kahramanmaraş, Göksun, Payanburnu mevki	PAY	<i>P. nigra</i>	10 / 17	S	1367	37°52'	36°21'
Artvin, Borçka, Balcı işletmesi	ART	<i>Abies nordmanniana</i> <i>Picea orientalis</i>	23 / 45	N	1200– 2100	41°18'	41°54'

648

649

650 Table 2. Summary statistics for the new chronologies developed by this study in Turkey.

Site Code	Total chronology			Common interval		
	Time span	1st year (*EPS > 0.85)	Mean sensitivity	Time span	Mean correlations: among radii /between radii and mean	Variance explained by PC1 (%)
KAR	1307– 2003	1620	0.22	1740–1994	0.38 / 0.63	41
SAH	1663– 2003	1738	0.25	1799–2000	0.42 / 0.67	45
ERC	1721– 2008	1721	0.23	1837–2008	0.45 / 0.69	48
BOL	1752– 2009	1801	0.18	1839–1994	0.32 / 0.60	36
SAV	1630– 2005	1700	0.17	1775–2000	0.33 / 0.60	38
HCR	1532– 2010	1704	0.18	1730–2010	0.38 / 0.63	40
PAY	1537– 2010	1790	0.18	1880–2010	0.28 / 0.56	32
ART	1498– 2007	1624	0.12	1739–1996	0.37 / 0.60	41

*EPS = Expressed Population Signal [Wigley et al., 1984]

651
652

653 Table 3. Principal components analysis statistics for the Turkey temperature reconstruction
654 model.

	Explained variance (%)	Correlation coefficients with		The chronologies represented by higher magnitudes** in the eigenvectors
		May–August PPT	March–April TMP	
PC1	46.57	0.65	0.19	KAR, KIZ, TEF, BON, USA, TUR, CAT, INC, ERC, YAU, SAV, TAN, SIU
PC2	7.86	–0.07	0.15	KAR, SAV, TIR, BOL, YAU, ESK, TEF, BON, SIU
PC3*	4.93	0.04	–0.48	HCR, PAY, BOL, YAU, SIA
PC4*	4.68	0.11	0.17	TEF, KEL, FIR, SIA, KIZ, SIU, ART
PC5*	4.42	–0.25	0.27	SAH, TIR, FIR, ART
PC6	3.73	0.15	–0.14	KIZ, FIR, SAV, KAR, TIR, PAY, ESK, TEF, BON, ART
PC7*	3.56	0.19	0.18	KIZ, BON, BOL, YAU, HCR, PAY, INC
PC8	2.87	0.26	0.01	HCR, ESK, BON, FIR, ERC, SIA
PC9*	2.45	0.16	0.17	PAY, USA, BOL, YAU, TIR, HCR, FIR, SIA, SIU
PC10*	2.21	0.14	–0.08	TUR, CAT, SAV, SIA, KEL, ERC, SIU
PC11	2.09	–0.36	–0.20	HCR, TEF, USA, INC, PAY, TUR, SAV, SIU
PC12	1.80	–0.12	0.05	TEF, CAT, YAU, HCR, ESK, USA, BOL, SIA
PC13	1.63	–0.06	0.17	TEF, TUR, BOL, KAR, YAU, SIA
PC14	1.55	–0.14	0.06	TIR, USA, FIR, TUR, YAU, KAR, BON
PC15*	1.50	–0.20	–0.14	KIZ, BON, USA, ESK, INC, BOL
PC16	1.31	0.04	0.08	SAH, HCR, INC, YAU, SAV, KAR, FIR, BOL, SIU
PC17*	1.25	0.15	0.19	SAH, SIU, KAR, ESK, TUR, ERC
PC18	1.14	0.13	0.02	KAR, TEF, TUR, SAV, BON, CAT
PC19	1.09	0.16	–0.11	PAY, INC, SAV, HCR, KEL, CAT, TAN
PC20	0.95	–0.15	–0.01	TIR, SAH, CAT
PC21*	0.89	0.06	–0.28	TUR, INC, TIR, SAV
PC22	0.85	0.44	0.10	KIZ, SAH, BON, YAU, SIU
PC23	0.67	–0.22	–0.02	TAN, KEL, TUR, CAT

655 “*” indicates the PCs, which used in the reconstruction as predictors

656 “**” which exceed ± 0.2 value.

657
658

659

660

661

662 Table 4. Calibration and verification statistics of bootstrap method (1000 iterations

663 applied) showing the mean values based on the 95% confidence interval (CI).

664

Mean (95% CI)		
Calibration	RMSE	0.65 (0.52; 0.77)
	R^2	0.73 (0.60; 0.83)
Verification	RE	0.54 (0.15; 0.74)
	CE	0.51 (0.04; 0.72)
	RMSEP	0.88 (0.67; 1.09)

665 *RMSE* root mean squared error; R^2 coefficient of determination; *RE* reduction of error; *CE*

666 coefficient of efficiency; *RMSEP* root mean squared error prediction

667

668 Table 5. Calibration and cross-validation statistics for the Turkey temperature reconstruction

669 model.

Calibration Period	Verification Period	Adj. R^2	F	RE	CE
1930–1966	1967–2002	0.55	5.91	0.64	0.58
$p < 0.0001$					
1967–2002	1930–1966	0.71	10.45	0.63	0.46
$p < 0.0001$					

670

671

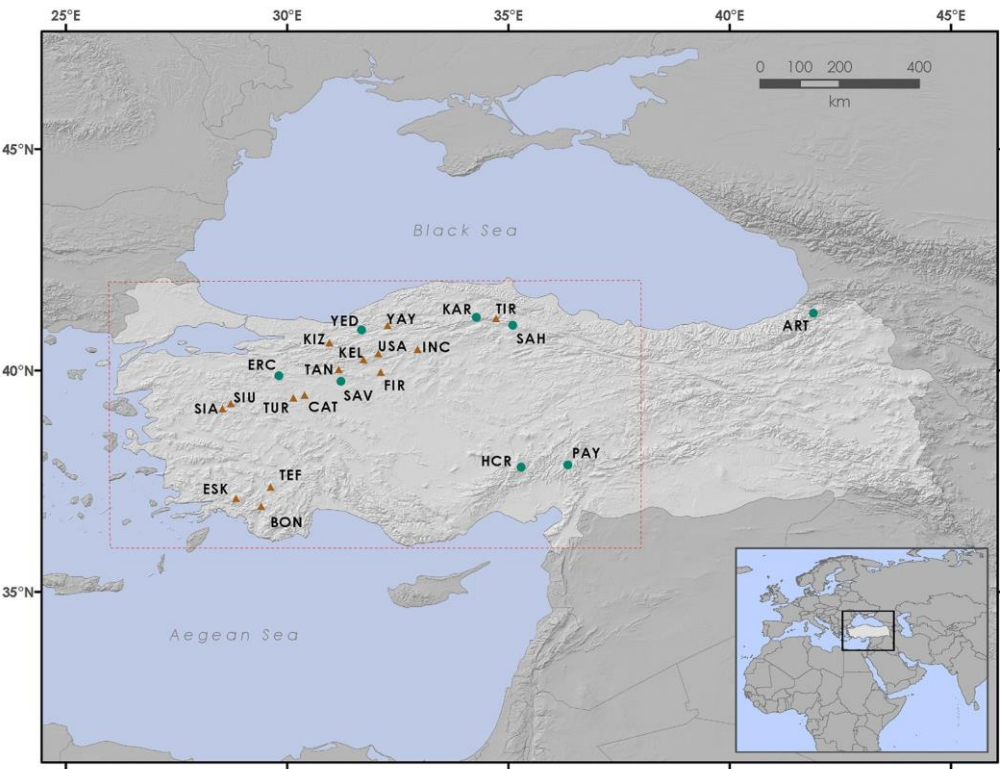


Figure 1. Tree-ring chronology sites in Turkey used to reconstruct temperature. Circles represent the new sampling efforts from this study and the triangles represent previously-published chronologies (YAY, SIA, SIU: Mutlu et al. 2011; TIR: Akkemik et al. 2008; TAN: Köse et al. unpublished data; KIZ, ESK, TEF, BON, KEL, USA, FIR, TUR: Köse et al. 2011; CAT, INC: Köse et al. 2005). The box (dashed line) represents the area for which the temperature reconstruction was performed.

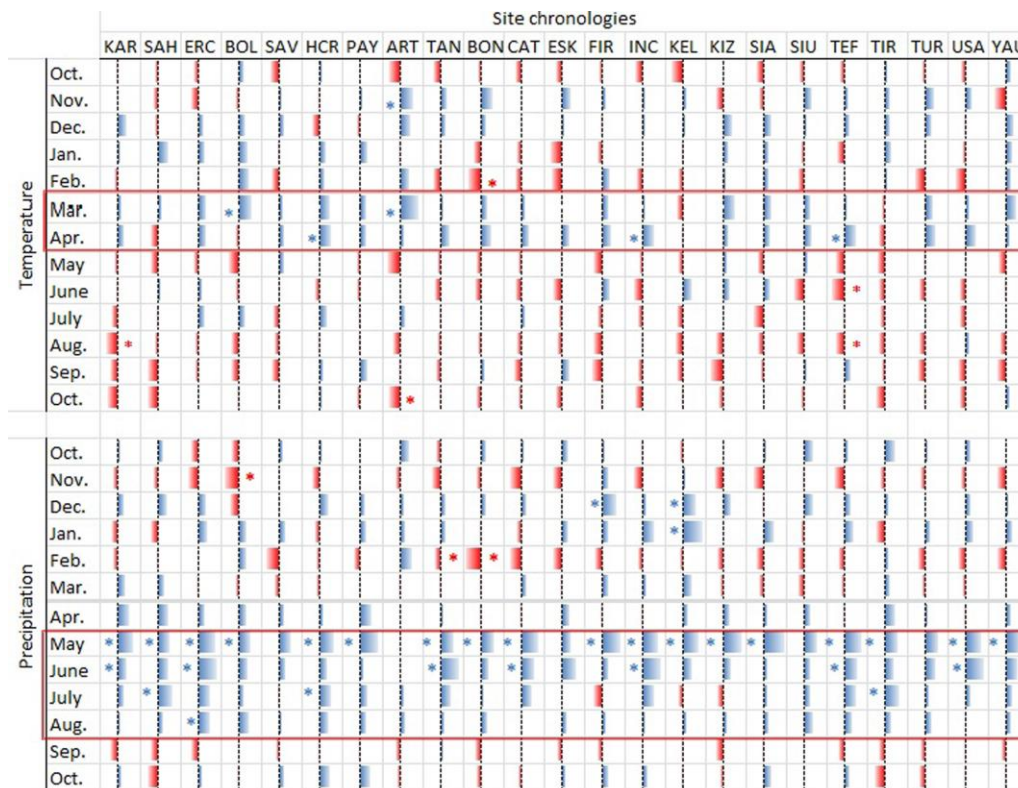


Figure 2. Summary of response function results of 23 chronologies. Red color represents negative effects of climate variability on tree ring width; blue color represents positive effects of climate variability on tree ring width. “*” indicates statistically significant response function confidants ($p < 0.05$). Each response function includes 13 weights for average monthly temperatures and 13 monthly precipitations from October of the prior year to October of current year.

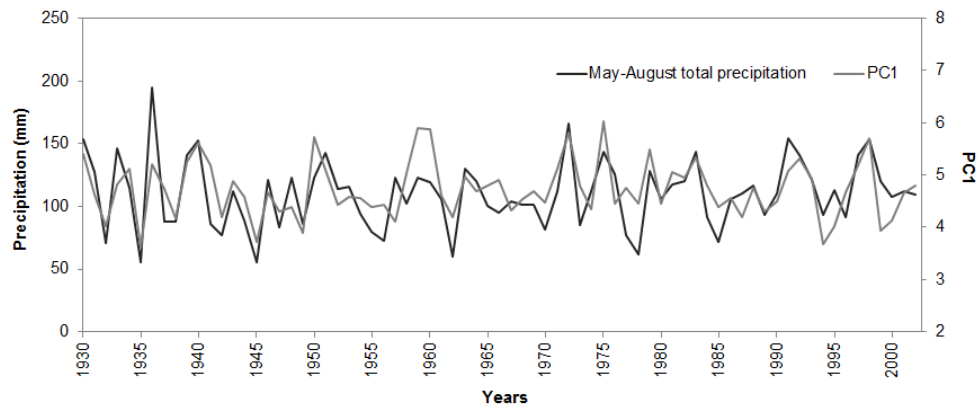


Figure 3. The comparison of May–August total precipitation (black) and the first principal component of 23 tree-ring chronologies (gray). Correlation coefficient between two time series is 0.65 ($p < 0.001$).

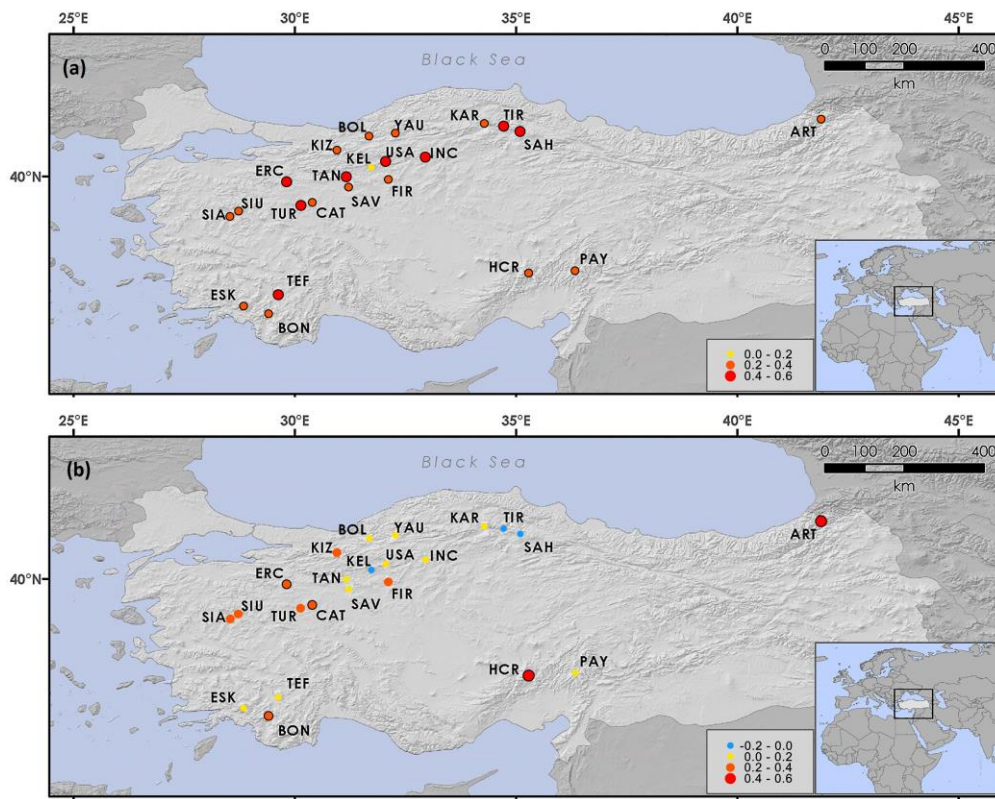
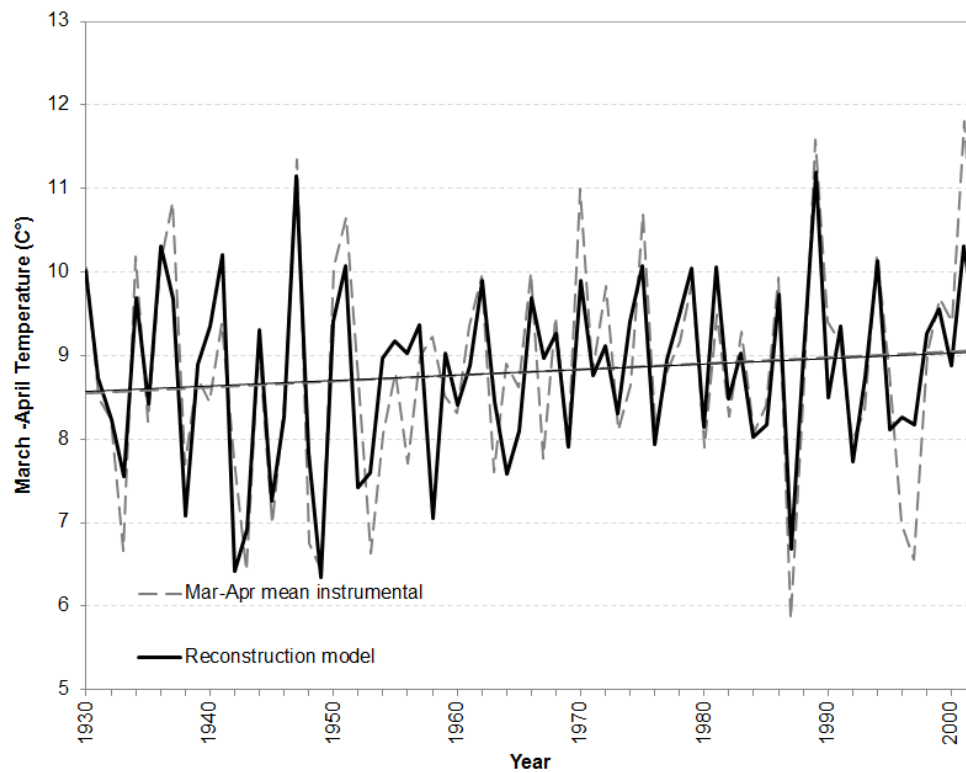


Figure 4. Maps showing Pearson's correlation coefficients between the sites chronologies and (a) May–August total precipitation and (b) March–April mean temperature for the period 1930–2012. For each site, the closest gridded ($0.5^\circ \times 0.5^\circ$) climate data obtained from CRU dataset were used. Graduated circle size and color correspond to correlation coefficient versus the climate variable. Black lines surrounding circles represent significant correlation coefficients ($p < 0.05$).

707



708

709 **Figure 5.** Actual (instrumental) and reconstructed March–April temperature (°C). Dashed lines
 710 (dark grey) represent actual values and solid lines (black) represent reconstructed values shown
 711 with trend lines (linear dashed grey and linear black lines, respectively). Note: y axes labels
 712 range 5–13 °C. The tendency to warm up at the reconstructed temperature is in good agreement
 713 with the trend in instrumental data.

714

715

716

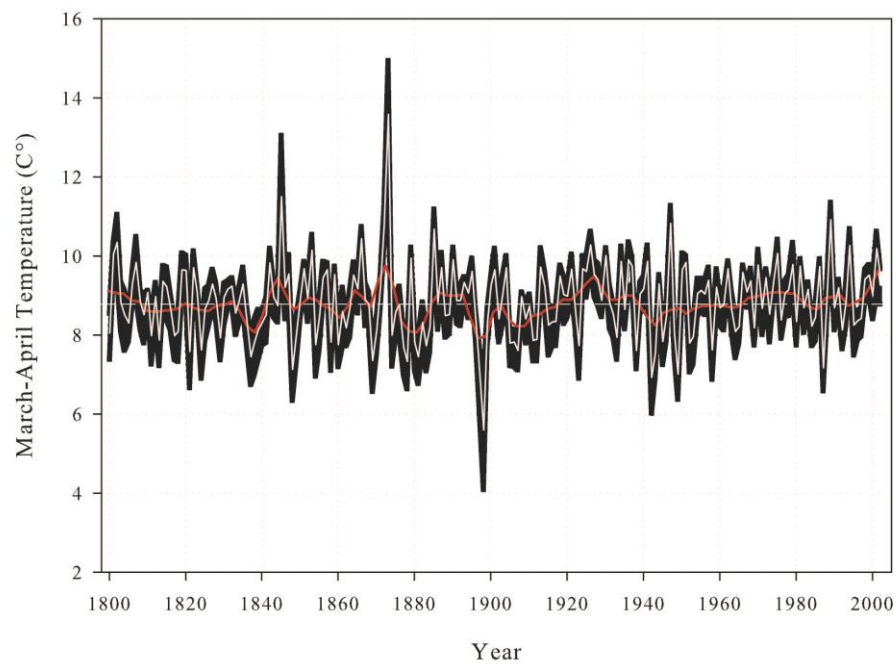


Figure 6. March–April temperature reconstruction for Turkey for the period 1800–2002 CE. The central horizontal line (dashed white) shows the reconstructed long-term mean [and does not include instrumental data](#); black background denotes Monte Carlo ($n = 1000$) bootstrapped 95% confidence limits; and the red line shows 13-year low-pass filter values. [Note: y axis labels range 2–16 °C.](#)

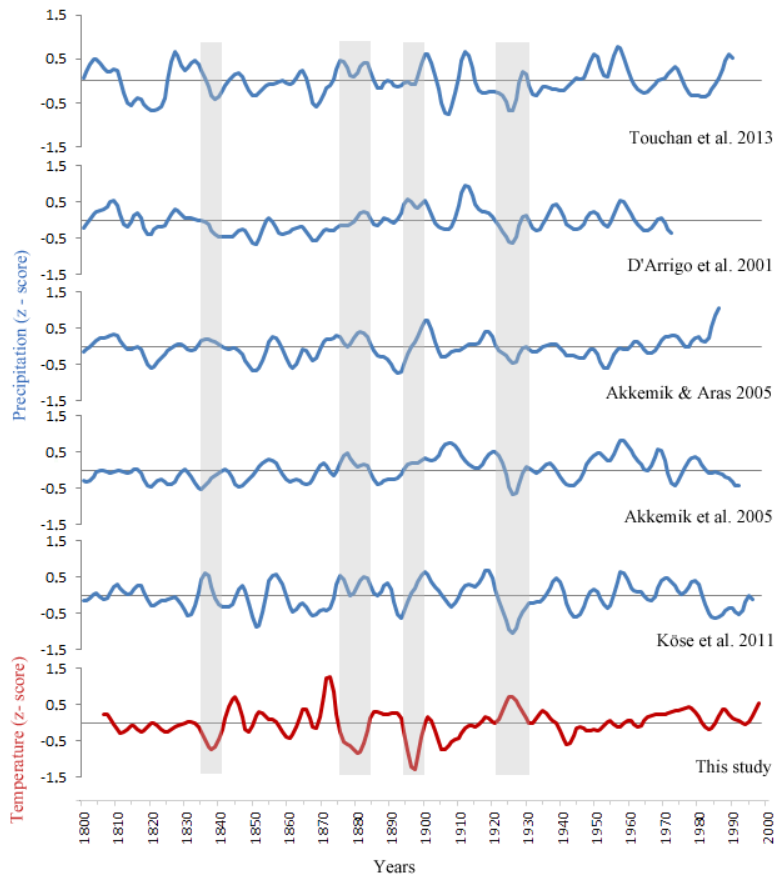
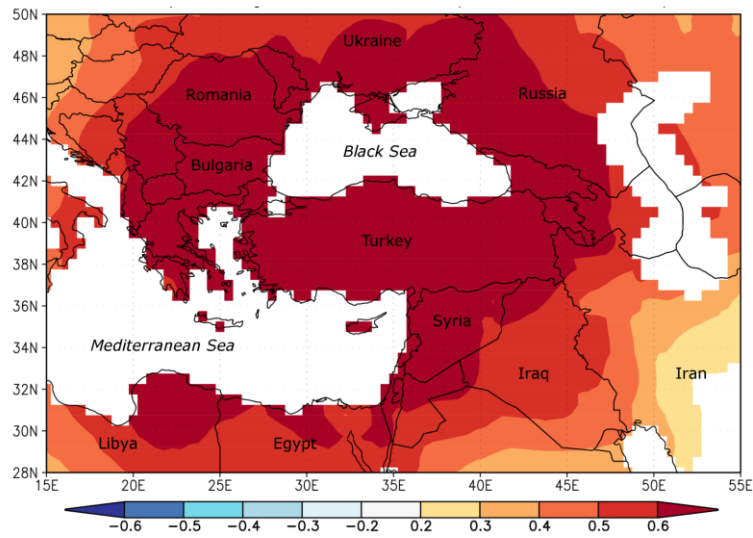


Figure 7. Low frequency variability of previous tree ring based precipitation reconstructions from Turkey and spring temperature reconstruction. Each line shows 13-year low pass filter values. z-scores were used for comparison.

Biçimlendirilmiş: Ortadan



736

737 | **Figure 78.** Spatial correlation map for the March–April temperature reconstruction. Spatial
 738 field correlation map showing statistical relationship between the temperature
 739 reconstruction and the gridded temperature field at 0.5° intervals (CRU TS3.23; Jones and
 740 Harris 2008) during the period 1930–2002 over the Mediterranean region. For each grid,
 741 calculated correlation coefficient from 0.20 to 0.60 is significant ($p < 0.05$).

742

(a) gridded spring temperature reconstruction for Europe (Xoplaki et al. 2005), (b) gridded summer temperature reconstruction for Europe (Luterbacher et al. 2016), (c) Old World Drought Atlas (OWDA; Cook et al. 2015). Panels (d) and (e) show spatial correlations between PC1 and OWDA (Cook et al. 2015) and gridded European summer precipitation reconstruction (Pauling et al., 2006), respectively. ‘+’ represents significant correlation coefficients ($p < 0.05$).

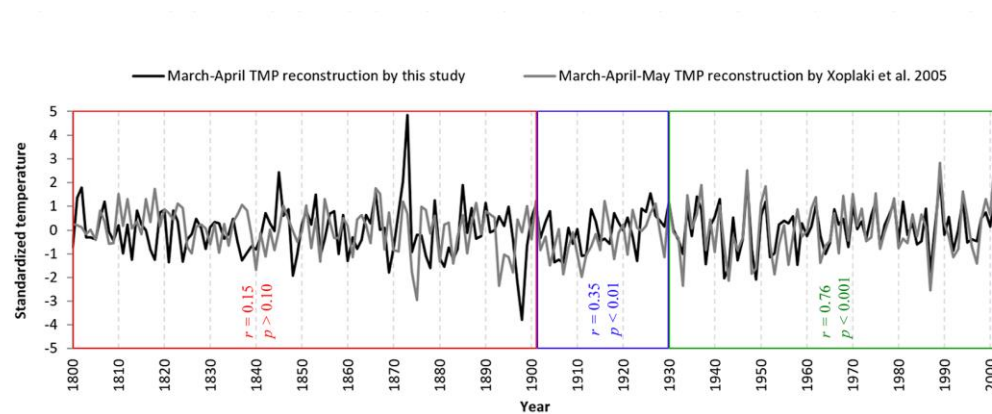


Figure 199. Comparison of March-April temperature reconstruction (gray) with the mean of corresponding grid points from European spring (March to May) temperature reconstruction (Xoplaki et al. 2005; black) over the study area (36–42° N, 26–38° E). The indicated correlation coefficients are calculated for instrumental period (also calibration period for this study) (1930–2002; $r = 0.76$, $p < 0.001$); for the pre-instrumental period of Turkey, while instrumental data has sufficient quality for most part of Europe (1901–1929; $r = 0.35$, $p < 0.10$); and for pre-instrumental period (1800–1900; $r = 0.13$, $p < 0.10$).